UASLP
Universidad Autónoma de San Luis Potosí

FACULTAD DE CIENCIAS

A STUDY ON COMBINATORICS OF LINK PROJECTIONS: REGULAR PROJECTIONS OF THE LINK L6N1 AND PROLIFICITY OF ARRANGEMENTS OF PSEUDOCIRCLES

Tesis que para obtener el grado de Doctor en Ciencias Interdisciplinarias

Presenta

Santino Ernesto Ramírez Medrano

Línea de Investigación

Modelamiento Matemático y Computacional

Director de Tesis

Dr. Gelasio Salazar Anaya, Universidad Autónoma de San Luis Potosí

San Luis Potosí, 13 de mayo de 2026

POSGRADO EN CIENCIAS INTERDISCIPLINARIAS

Instituto de Física

Abstract

The relationship between a link embedded in the 3-sphere and its planar projection (or shadow) is a central subject in knot theory. This thesis investigates two distinct facets of this relationship. First, we address the characterization problem: for a particular link L, a fundamental problem consists of characterizing the exact set of shadows that are projections of L. While this question has been resolved for links with small crossing numbers, we extend this inquiry to the 3-component prime link $L6n1$. This work provides a complete characterization: any 3-component link projection is in fact a projection of $L6n1$ under the necessary and sufficient condition that its components intersect pairwise. This is achieved through the identification and analysis of reduction operations that simplify projections while preserving key properties, ultimately characterizing the irreducible projections of $L6n1$.

Second, we explore the prolificity of shadows: what is the total number of distinct links that can be obtained from a particular shadow? We focus specifically on shadows formed by arrangements of pseudocircles (collections of Jordan curves that pairwise intersect exactly twice) and restrict our analysis to the realization of positive oriented links. We establish precise asymptotic bounds for the number of distinct positive oriented links that can be obtained over the three unavoidable classes of pseudocircle arrangements: the ring $\mathscr{R}_n$, the boot $\mathscr{B}_n$, and the flower $\mathscr{F}_n$. We demonstrate that the number of such links, relative to the total number of possible positive realizations (2^n), behaves asymptotically as $1/4$ for $\mathscr{R}_n$, 1 for $\mathscr{B}_n$, and $1/(2n)$ for $\mathscr{F}_n$.

Acknowledgments

In the first instance, I owe my deepest gratitude to my wife for her understanding, love, and unconditional support during my PhD. Her encouragement was a fundamental pillar in achieving this goal.

To my sisters, Marisol and Karina, I sincerely thank you for always being there for me and for caring about me throughout all these years of study. Without you, this achievement would not have been possible.

I am profoundly indebted to my doctoral advisor, Dr. Gelasio Salazar, for his exceptional mentorship, unwavering integrity, and strict mathematical rigor. His feedback and vision were crucial to the development and culmination of this work.

I extend my sincere appreciation to the members of my thesis committee. Their careful reading, perceptive critiques, and valuable suggestions have substantially elevated the rigor and clarity of this manuscript. I would like to extend a special acknowledgment to Dr. Edgardo Ugalde for his continuous guidance in my academic development and for his invaluable assistance in making my academic visit to Marseille possible. Furthermore, I am deeply thankful to SECIHTI for their generous financial backing throughout the course of my doctoral studies.

Lastly, I thank my family, professors, and colleagues who accompanied me throughout my entire academic journey.

Contents

Part I

Introduction and Background

Chapter 1

Introduction

Throughout this manuscript, we work in the piecewise linear category. For any link L embedded in $\mathbb{S}^3$, projecting it onto $\mathbb{S}^2$ (or $\mathbb{R}^2$) yields the projection, or shadow, of the link. This shadow is typically viewed as a 4-regular graph, where the crossings of the projection are treated as vertices. By assigning over/under information at each crossing, we *resolve* the shadow, resulting in a link *diagram*, we refer to [2] for standard knot theory terms and background.

A fundamental inquiry in knot theory concerns the connection between a link and its possible shadows. This thesis explores two primary questions stemming from this relationship:

1. **Characterization:** for a particular link L, a fundamental problem consists of characterizing the exact set of shadows that are projections of L.
2. **Prolificity:** what is the total number of distinct links that can be obtained from a particular shadow?

1.1 The Characterization Problem

Given a shadow P and a link L, determining if P is a projection of L is a well-studied problem [3,6,9,10,13–17,20,21,28–30]. Taniyama provided comprehensive answers for all prime links (including knots) with crossing numbers up to five [32, 33]. More recently, Takimura addressed the knot 6_2 [31].

The first part of this thesis addresses this question for the 3-component prime link $L6n1$ [1]. We provide a complete characterization of the planar shadows that arise as regular projections of the 3-component link $L6n1$. We define a projection P composed of three components (colored blue B, red R, and green G) as *pairwise crossing* if all the curves mutually intersect. It is a direct consequence of $L6n1$ being pairwise linked that its shadows must necessarily be pairwise crossing. As a central result, we demonstrate the sufficiency of this condition.

Theorem 1.1. *([3]) Let P be a projection of a link with three components. Then P is a projection of the link $L6n1$ if and only if it is pairwise crossing.*

The proof strategy involves defining reduction operations on shadows that simplify the structure while preserving the set of realized links. We characterize the *irreducible* projections those that cannot be further reduced and show that they are all projections of $L6n1$.

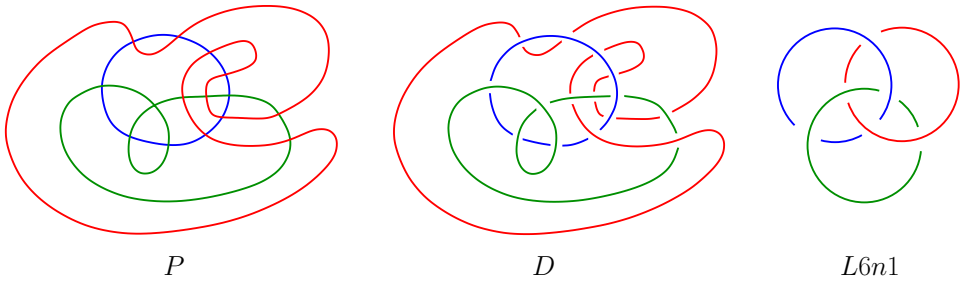

Figure 1.1: Starting with a 3-component link projection P (left), we construct the central diagram D by specifying a crossing assignment for each intersection. Applying a sequence of Reidemeister transformations reduces D to the configuration on the right, a recognized diagram of $L6n1$. Consequently, this sequence proves that P is a shadow of the link $L6n1$.

1.2 The Prolificity Problem

The second question investigates the diversity of links arising from a single shadow. This concept is related to *fertility* [7, 17, 18, 22], also, the relationship between shadows and the *unknotting number* of a link diagram is explored in [25]. Quantifying the exact number of non-equivalent links that realize an arbitrary shadow S with n crossings presents a significant challenge, as it involves analyzing the 2^n possible diagrams arising from S and determining their equivalence classes.

We narrow the scope of this investigation by focusing on a specific family of shadows: *arrangements of pseudocircles*. By an arrangement of pseudocircles of size n, we refer to a set of n Jordan curves such that each pair crosses transversally in exactly two distinct points. Furthermore, we restrict our analysis to *positive* links, where all crossings in the diagram adhere to the positive convention.

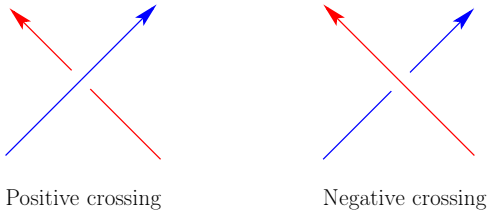

Figure 1.2: The convention for positive and negative crossings.

We primarily investigate oriented links. Every oriented arrangement straightforwardly determines a unique positive link diagram. Given an unoriented arrangement of n pseudocircles $\mathscr{A}$, there are 2^n ways to orient the components, yielding 2^n positive oriented links, denoted by the collection $\overrightarrow{\mathcal{L}}^+(\mathscr{A})$. We aim to determine $[\![\overrightarrow{\mathcal{L}}^+(\mathscr{A})]\!]$, the cardinality of the set of non-equivalent links within $\overrightarrow{\mathcal{L}}^+(\mathscr{A})$.

We focus on the three *unavoidable* families of arrangements [26]: the ring arrangement $\mathscr{R}_n$, the boot arrangement $\mathscr{B}_n$, and the flower arrangement $\mathscr{F}_n$. The fundamental importance of these families stems from the fact that any pseudocircle arrangement of sufficient size necessarily admits a subarrangement that is isomorphic to at least one of them.

Our main results [27] in this area provide asymptotic estimates for the prolificity of these unavoidable arrangements.

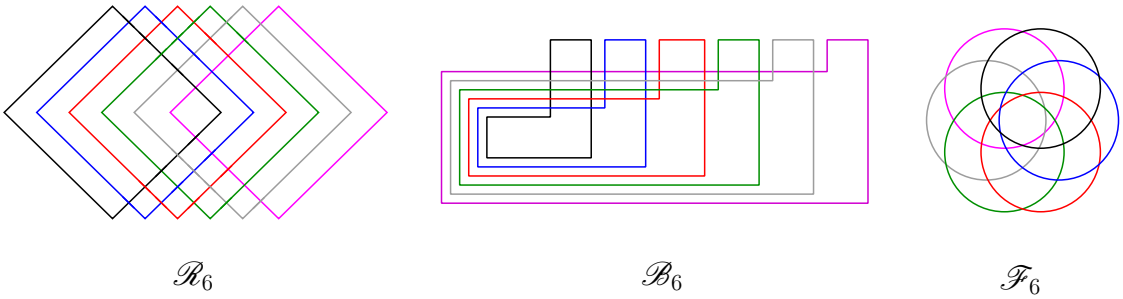

$\mathscr{R}_6$ $\mathscr{B}_6$ $\mathscr{F}_6$

Figure 1.3: The three unavoidable arrangements on six curves: from left to right, we illustrate the ring $\mathscr{R}_6$, the boot $\mathscr{B}_6$, and the flower $\mathscr{F}_6$ arrangements.

Theorem 1.2 (Ring Arrangement). $[\![\overrightarrow{\mathcal{L}}^+(\mathscr{R}_n)]\!] = \left(\frac{1}{4} + o(n)\right) \cdot 2^n$.

Theorem 1.3 (Boot Arrangement). $[\![\overrightarrow{\mathcal{L}}^+(\mathscr{B}_n)]\!] = \left(1 + o(n)\right) \cdot 2^n$.

Theorem 1.4 (Flower Arrangement). $[\![\overrightarrow{\mathcal{L}}^+(\mathscr{F}_n)]\!] = \left(\frac{1}{2n} + o(n)\right) \cdot 2^n$.

These results indicate that the boot arrangement is highly prolific (almost every orientation yields a unique link), whereas the ring and flower arrangements exhibit more symmetry, leading to larger equivalence classes.

1.3 Motivation

In a seminal series of papers [32, 33], Taniyama introduced a partial order on the set of prime knots. We define a knot K_1 to be a minor of another knot K_2, denoted by $K_1 \leqslant K_2$, if the collection of all projections of K_2 constitutes a subset of those of K_1. This definition formalizes the intuitive notion of "complexity" in terms of shadows: if every shadow capable of representing K_2 is also capable of representing K_1, then K_1 is in some sense simpler or more fundamental.

To compute this partial order, one must first solve the Characterization Problem for specific knots. Taniyama successfully characterized the projections of all prime knots with crossing numbers up to 5. To illustrate this, he demonstrated that a regular projection corresponds to the trefoil knot under the necessary and sufficient condition that it avoids having exclusively cut vertices. More recently, Takimura [31] extended this analysis to the knot 6_2, using sophisticated local moves.

However, the theory for multi-component links is less developed. While the definition of Taniyama's order extends naturally to links, the combinatorial constraints imposed by multiple components specifically the interactions between them add layers of complexity. The link $L6n1$, being a 3-component link with non-trivial linking numbers between all pairs of components (it is pairwise linked), represents a significant leap in difficulty. Understanding $L6n1$ requires tracking not just the self-crossings of components, but the "mixed" crossings that define the linking structure. Our work in this thesis fills this gap, providing the first complete characterization for a prime link of this complexity and subsequently determining its place in the Taniyama lattice.

While the Characterization Problem fixes the link and varies the shadow, the Prolificity Problem fixes the shadow and asks about the diversity of links it can come from. This line of inquiry is motivated by the search for "universal" or "fertile" shadows. A shadow is termed

universal if it can represent every knot [11].

While universality focuses on the existence of specific links, *prolificity* (or fertility density) focuses on the quantity. If we randomly resolve the crossings of a shadow with n vertices, we generate 2^n diagrams. How many distinct isotopy classes of links do these diagrams represent?

Counting these classes is computationally hard for general graphs due to the difficulty of the link equivalence problem. However, by restricting the class of shadows to *arrangements of pseudocircles* and the class of links to *positive links*, the problem becomes tractable via combinatorial group theory. Arrangements of pseudocircles are of particular interest in discrete geometry; a theorem by Medina, Ramírez-Alfonsín, and Salazar [26] states that any sufficiently large arrangement must contain specific sub-structures: the Ring, Boot, or Flower arrangements. These are the "atoms" of large arrangements. By determining the prolificity of these unavoidable families, we take a crucial step toward understanding the asymptotic diversity of links in large, random geometric graphs.

1.4 Reduction Operations and Irreducibility

To characterize the projections of $L6n1$, we employ a strategy of *graph reduction*. We define local operations on 4-regular graphs that reduce the number of vertices while preserving the property of being a projection of $L6n1$.

1. **Shortcutting:** This operation removes a loop or a redundant path in the graph, effectively simplifying a component that does not interact significantly with others in a local region.
2. **Θ-Simplification:** This operation collapses a specific digon structure, simplifying the interaction between two strands.

The core of our proof lies in determining the base cases of this reduction process. We define a projection to be *irreducible* if no reduction operations can be applied. We then prove a structural theorem: there are exactly two non-equivalent irreducible projections (up to equivalence) with the pairwise crossing condition. By verifying that both irreducible projections can resolve to $L6n1$, and proving that the reduction operations preserve the resolution onto the link $L6n1$, we establish the characterization theorem.

1.5 Binary Words and Symmetry Groups

For the analysis of Ring, Boot, and Flower links, we translate the topological problem into a combinatorial one. Each of these arrangements consists of n ordered (or cyclically ordered) curves. A positive link diagram on such an arrangement is fully determined by the orientation of each curve. Thus, we establish a canonical one-to-one correspondence between the collection of these links and the space of binary words of length n (where 0 and 1 represent clockwise/counter-clockwise orientation).

Consequently, the counting of distinct link isotopy classes translates directly into calculating the number of orbits of binary words under the action of the arrangement's *intrinsic symmetry group*.

- For **Ring links**, the symmetries allow for reversing the word and taking the bitwise complement, corresponding to spatial rotations of the link.
- For **Flower links**, the cyclic nature of the arrangement introduces dihedral symmetries (cyclic shifts).

- For **Boot links**, the lack of symmetry means almost every word corresponds to a unique link.

We prove these equivalences rigorously by analyzing the *rank* of the binary words (the length of the longest alternating subword) and using inductive arguments on sub-links. This allows us to deduce precise asymptotic formulas for the number of unique links as $n \to \infty$.

1.6 Thesis Outline

The overall structure of this thesis is delineated as follows:

Chapter 2 provides the necessary prelude, defining links, shadows, diagrams, and the graph-theoretical terminology used throughout the work. We formally define pairwise crossing projections and arrangements of pseudocircles.

Part II focuses on the regular projections of the link $L6n1$.

- **Chapter 3** introduces the reduction operations shortcutting and simplifying a Θ operation and proves their key property: that the set of links realizable by a reduced projection is a subset of those realizable by the original.
- **Chapter 4** is devoted to the structural analysis of irreducible projections. We prove that any irreducible pairwise crossing projection must be isomorphic to one of two specific graphs with 6 vertices.
- **Chapter 5** presents the proof of the main characterization theorem for $L6n1$. We also apply this result to the Taniyama partial order, identifying the majors and minors of $L6n1$.

Part III focuses on positive links induced by arrangements of pseudocircles.

- **Chapter 6** sets the stage for the asymptotic analysis, defining the correspondence between oriented arrangements and binary words.
- **Chapter 7** analyzes Ring links. We establish the isomorphism between Ring links and binary words under the action of the Klein four-group ($\mathbb{Z}_2 \times \mathbb{Z}_2$).
- **Chapter 8** extends this analysis to Flower links, dealing with the more rich dihedral symmetry group D_n.
- **Chapter 9** treats Boot links, demonstrating their lack of intrinsic symmetries and establishing their high prolificity.

Finally, **Chapter 10** offers our conclusions and discusses various directions for future research.

Chapter 2

Preliminaries

In this chapter we introduce the fundamental definitions and notation used throughout the thesis. We adopt a graph-theoretical perspective for analyzing link projections.

2.1 Links, Projections and Diagrams

We consider links embedded in $\mathbb{S}^3$. In our analysis, we formally treat link projections as 4-regular graphs that are topologically embedded within the 2-sphere $\mathbb{S}^2$. This is achieved by interpreting each crossing in the projection as a vertex of degree 4. See Figure 2.1.

Definition 2.1. ([3]) By a *link diagram* of L, we refer to a regular planar or spherical projection where the components are smooth and intersect only at transverse double points, and over/under information is specified at each crossing. A projection is classified as *regular* provided that its intersections consist exclusively of a finite number of transverse double points.

Definition 2.2. ([3]) A *link* projection (or *shadow*) is precisely the 4-regular plane graph that results from forgetting the crossing information of a given link diagram.

Definition 2.3. ([3]) Two projections are deemed equivalent provided there exists a self-homeomorphism of the 2-sphere $\mathbb{S}^2$ that maps one onto the other. Furthermore, all links are considered strictly up to ambient isotopy.

Definition 2.4. ([3]) A projection P *is a projection of* L if there exists a link isotopic to L that projects to P. Equivalently, P is a projection of L if P can be resolved to obtain a diagram D of a link isotopic to L.

Following the notation introduced in [30] and [32]:

Definition 2.5. ([3]) For a given shadow P, we let $\textsc{Link}(P)$ denote the set of all links L that admit P as a projection.

Under this terminology, Theorem 5.1 demonstrates the following equivalence: given a 3-component projection P, the condition $L6n1 \in \textsc{Link}(P)$ holds if, and only if, P is a pairwise crossing projection.

2.2 Straight-Ahead Walks and Coloring

Definition 2.6. ([3]) Within a 4-regular graph, a *straight-ahead walk* is defined as a sequence of edges such that, upon entering any vertex v, the traversal strictly continues along the edge situated directly opposite to the incoming edge. We define a walk to be *closed* if it originates and terminates at the exact same vertex.

We focus on projections of 3-component links. Consequently, throughout this analysis, any given projection P admits a complete decomposition into three edge-disjoint, straight-ahead closed walks. Specifically, we express P as the union $P = B \cup R \cup G$, corresponding to a blue component B, a red component R, and a green component G.

Definition 2.7. ([3]) We say that a projection $P = B \cup R \cup G$ is *pairwise crossing* if every pair of its constituent walks shares at least one intersection.

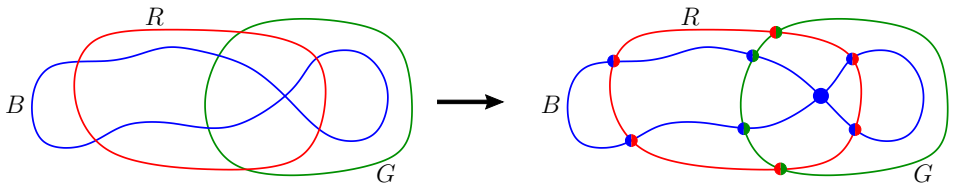

Figure 2.1: A projection P is decomposed into its constituent straight-ahead closed walks blue (B), red (R), and green (G), and regarded as a 4-regular graph. The configuration is pairwise crossing, as evidenced by the existence of at least one crossing vertex for each color pair.

2.3 Vertex Classification

Vertices are classified based on the colors of the incident edges.

Definition 2.8. ([3]) We classify a vertex v as *monochromatic* when the set of four edges incident to it are identically colored. The vertex is colored accordingly (blue, red, or green).

Definition 2.9. ([3]) A vertex v of P is *bichromatic* if two incident edges are of one color and the other two are of a different color. The vertex is colored with both colors. Bichromatic vertices are categorized into three distinct types according to their incident color pairs: blue-red, red-green, and blue-green.

In a pairwise crossing projection, the Jordan curve theorem implies that there must be at least two vertices for each bichromatic type (e.g., at least two green-red vertices, as G and R must cross each other at least twice).

2.4 Arrangements of Pseudocircles

In the context of Part III, we focus on specific types of shadows.

Definition 2.10. ([27]) A collection of n Jordan curves in the plane is considered an *arrangement of pseudocircles* of size n if every pair of curves within the collection intersects transversally at exactly two distinct points.

Endowing each pseudocircle with an orientation naturally yields an *oriented arrangement*.

2.4.1 Positive Links

Definition 2.11. ([27]) A link is classified as *positive* if it admits a diagram in which every crossing is positive (following the convention in Figure 1.2).

Every oriented arrangement canonically defines a positive link by assigning over/under information at each crossing to ensure it is positive.

2.4.2 Unavoidable Arrangements

We study three specific families of arrangements (illustrated in Figure 1.3 for $n = 6$): the *ring* arrangement $\mathscr{R}_n$, the *boot* arrangement $\mathscr{B}_n$, and the *flower* arrangement $\mathscr{F}_n$. These are *unavoidable* because every sufficiently large arrangement contains one of them as a subarrangement [26].

2.5 Isotopies and Symmetries

We use the term *isotopy* to mean ambient isotopy.

Definition 2.12. ([27]) We say that oriented links L and M are equivalent, written $L \sim M$, if they are isotopic under a deformation that respects the chosen orientation of each individual component. The expression $\mathcal{I} \,\big|\, L \to M$ is employed to indicate that $\mathcal{I}$ is the specific isotopy mapping L onto M, referred to as an $L \mapsto M$ isotopy.

When the components of links L and M are ordered ($L_1, \ldots, L_n$ and $M_1, \ldots, M_n$), an $L \mapsto M$ isotopy $\mathcal{I}$ induces a permutation π of $[n] = \{1, \ldots, n\}$, where $\mathcal{I} \,\big|\, L_i \to M_{\pi(i)}$. We say π *is the* (L, M)*-permutation under* $\mathcal{I}$, and write $\mathcal{I} \,\big|\, L \xrightarrow{\pi} M$.

Definition 2.13. ([27]) When π coincides with the identity permutation ι, ensuring that each component's index is strictly preserved, we refer to the deformation as a *strong* $L \mapsto M$ isotopy.

We establish the notation ν to designate the *reverse* permutation, $\nu(i) = n - i + 1$.

Observation 2.14. *([27]) Suppose we have two isotopies:* $\mathcal{I} \,\big|\, L \xrightarrow{\pi} M$ *and* $\mathcal{J} \,\big|\, M \xrightarrow{\tau} N$. *Consequently,* $\mathcal{J} \circ \mathcal{I}$ *represents an isotopy where* $\mathcal{J} \circ \mathcal{I} \,\big|\, L \xrightarrow{\tau \circ \pi} N$.

2.5.1 Intrinsic Symmetry Groups

We briefly introduce the concept of intrinsic symmetry, used in the analysis of oscillating links in Part III. Let $\mathbb{Z}_2 = \{-1, 1\}$. For a given oriented knot K, we denote by $-K$ the same underlying knot endowed with the strictly reversed orientation. Let $L = L_1 \cup \cdots \cup L_n$ be an oriented link.

Definition 2.15. ([27]) We say that a link L admits the intrinsic symmetry $(1, \epsilon_1, \ldots, \epsilon_n, \pi)$, where $\epsilon_i \in \mathbb{Z}_2$ and $\pi \in S_n$, provided there exists a self-isotopy of L that maps each component L_i to $\epsilon_i L_{\pi(i)}$.

The set of intrinsic symmetries forms the *intrinsic symmetry group* of L [35]. (We omit the definition involving mirror images as it is not relevant for positive links).

Part II

Regular Projections of the Link L6n1

Chapter 3

Reduction Operations and Irreducibility

A cornerstone of the proof of Theorem 5.1 is the utilization of two distinct *reduction operations* applied on link shadows. These operations simplify the structure of a projection while preserving essential properties.

3.1 Properties of Reduction Operations

Applying a reduction operation to a pairwise crossing projection P yields a resulting projection P' that fulfills the following conditions [3]:

(R1) *P' contains fewer vertices than P.*

(R2) *P preserves the property of being pairwise crossing.*

(R3) $\textsc{Link}(P') \subseteq \textsc{Link}(P)$. *(The set of links projected by P' is a subset of those projected by P).*

Definition 3.1. ([3]) A pairwise crossing projection P is classified as *irreducible* provided that it admits no further reduction operations.

Starting from an arbitrary pairwise crossing projection P, the iterative application of reduction operations must inevitably terminate in an irreducible projection P'. Due to property (R3), $\textsc{Link}(P') \subseteq \textsc{Link}(P)$. Therefore, if it is established that P' is a projection of $L6n1$, it logically follows that the antecedent projection P is also a projection of $L6n1$. Consequently, to establish Theorem 1.1 [3], it suffices to prove that all irreducible projections are in fact projections of the link $L6n1$.

3.2 The First Reduction Operation: Shortcutting a Projection

Consider a pairwise crossing projection denoted by $P = B \cup R \cup G$. Suppose there exists a face f bounded by at least two edges, e and e', sharing the same color class (without loss of generality, let this color be blue). This specific configuration is depicted in Figure 3.1(i), where the shaded region represents f and the thickened lines indicate e and e'.

By subdividing the edge e with a degree-2 vertex x and the edge e' with a degree-2 vertex y (see Figure 3.1(ii)), the original blue straight-ahead closed walk B naturally partitions into two distinct straight-ahead walks, denoted B_1 and B_2, both originating at x and terminating at y (Figure 3.1(iii) and (iv) [3]). These are referred to as the *xy-walks*.

Definition 3.2. ([3]) For each $i \in \{1, 2\}$, we define the walk B_i to be *colourful* provided that it traverses at least one blue-red vertex and at least one blue-green vertex.

In any case that B_1 or B_2 is colourful (assume B_1 is colourful, as in Figure 3.1) [3], we can *shortcut* B. This involves discarding B_2 and connecting x and y in B_1 with an arc contained within f (Figure 3.1(v)). At last, we remove the vertices x and y. This procedure ultimately yields a newly formed blue straight-ahead closed walk, denoted by $\overline{B}$ (Figure 3.1(vi)). We say that the modified projection $\overline{P} = \overline{B} \cup R \cup G$ is generated by *shortcutting* [3] the original projection P at x and y.

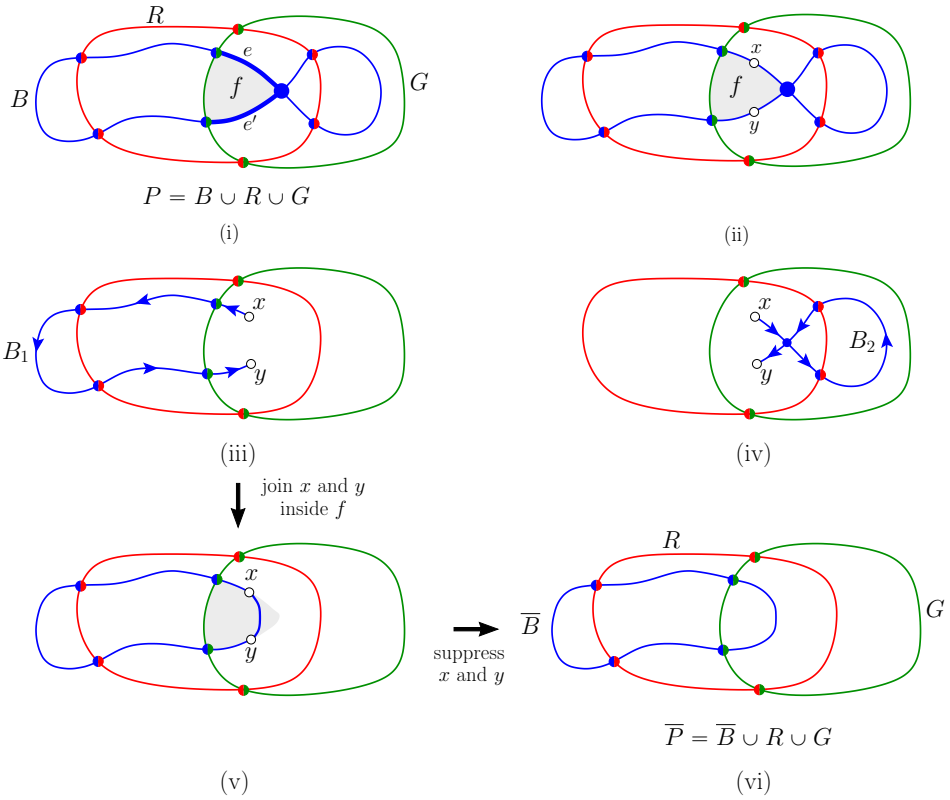

Figure 3.1: The shortcut operation.

Verification of Properties (R1)–(R3) for Shortcutting

Condition (R1) is satisfied since the internal vertices belonging to the discarded walk B_2 exist in the original projection P but are strictly excluded from the modified projection $\overline{P}$. (R2) holds because the colourfulness of B_1 ensures that $\overline{P}$ remains pairwise crossing. To verify (R3), we must show that if $L \in \text{LINK}(\overline{P})$, then $L \in \text{LINK}(P)$. Assume $\overline{P}$ is resolved into a diagram $\overline{D}$ of L. We need to construct a resolution of P into a diagram D equivalent to $\overline{D}$.

For vertices in P that are also in $\overline{P}$, we use the same resolution as in $\overline{D}$. For vertices in P that are not in $\overline{P}$ (i.e., the vertices on the discarded walk B_2), we employ the *descending algorithm* (as used in [30] and [32]). We traverse B_2 from x to y. Upon first encountering a vertex, we resolve it such that the strand being traversed is the overstrand. See Figure 3.2.

The execution of the descending algorithm [3] ensures that the strand connecting x to y within D is ambient isotopic to the corresponding strand in $\overline{D}$. Therefore, we deduce that D and $\overline{D}$ constitute equivalent link diagrams, confirming (R3). This operation can analogously be applied to the red or green walks.

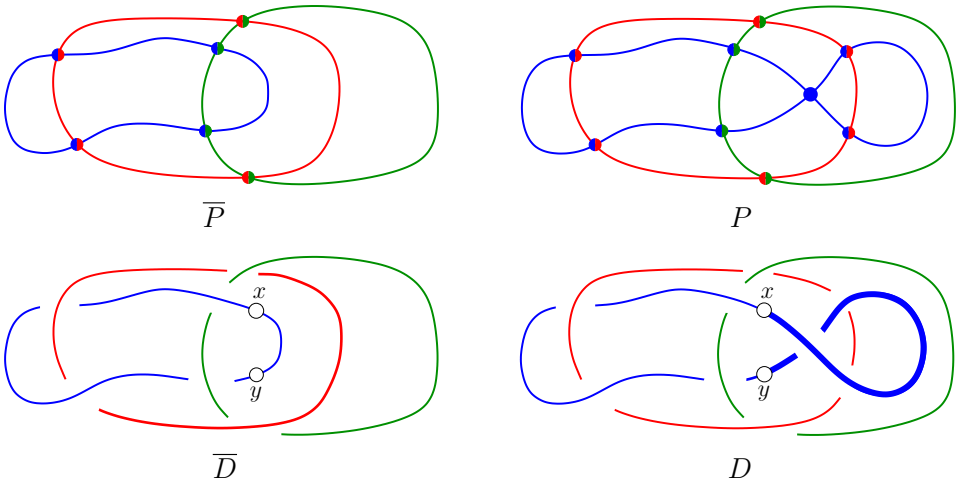

Figure 3.2: Through the application of the descending algorithm, a diagram $\overline{D}$ corresponding to the projection $\overline{P}$ can be systematically extended to yield a equivalent diagram D of P.

3.3 The Second Reduction Operation: Simplifying a Θ

Assume that the projection $P = B \cup R \cup G$ admits a straight-ahead cycle denoted by $C = uvwu$, a configuration depicted in Figure 3.3(i) [3].

Definition 3.3. ([3]) We define $C + e$ to be a Θ in P provided that two conditions hold: (a) the vertices v and w are joined by an edge e that is distinct from their connecting edge within C; and (b) the connected component of $\mathbb{S}^2 \backslash C$ in which e resides contains no other elements of the projection P. This configuration is illustrated in Figure 3.3(ii).

Figure 3.3: The concept of a Θ in a projection.

We *simplify* [3] the Θ configuration by *splitting* the vertex u, the procedure is detailed in Figure 3.4.

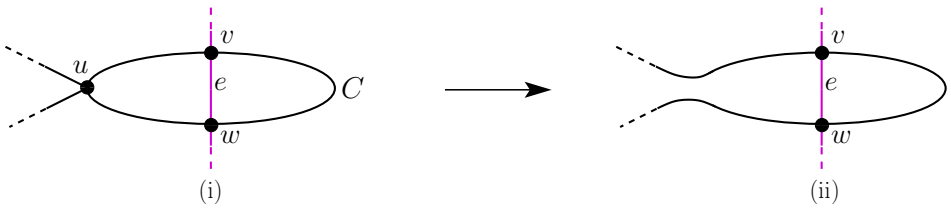

Figure 3.4: Simplifying a Θ by splitting the vertex u.

Verification of Properties (R1)–(R3) for Simplifying a Θ

Condition (R1) is satisfied since the modified projection $\overline{P}$ contains exactly one fewer vertex than P due to the elimination of u. Furthermore, (R2) holds because the straight-ahead nature

of the cycle C dictates that u must be monochromatic. Consequently, every bichromatic vertex present in P is strictly preserved in $\overline{P}$, ensuring that the pairwise crossing property remains an invariant of the projection.

To verify (R3), assume that $L \in \textsc{Link}(\overline{P})$, which implies that $\overline{P}$ admits a resolution into a diagram $\overline{D}$ representing the link L. We must demonstrate that P similarly resolves into an equivalent diagram D. To construct D, all vertices of P excluding $\{u, v, w\}$ are resolved identically to their counterparts in $\overline{D}$. The specific crossing resolutions assigned to u, v, and w within P are then entirely determined by the corresponding resolutions of v and w in $\overline{P}$.

Figure 3.5 delineates the four permissible resolution states for v and w within $\overline{P}$ (panels (i), (iii), (v), and (vii)) alongside their induced resolutions for u, v, and w in P (panels (ii), (iv), (vi), and (viii)). For each configuration, the strand connecting x to y in D admits an isotopy to the corresponding strand in $\overline{D}$. Because all remaining vertices share identical resolutions, the constructed diagram D is topologically equivalent to $\overline{D}$. This observation concludes the verification of (R3) [3].

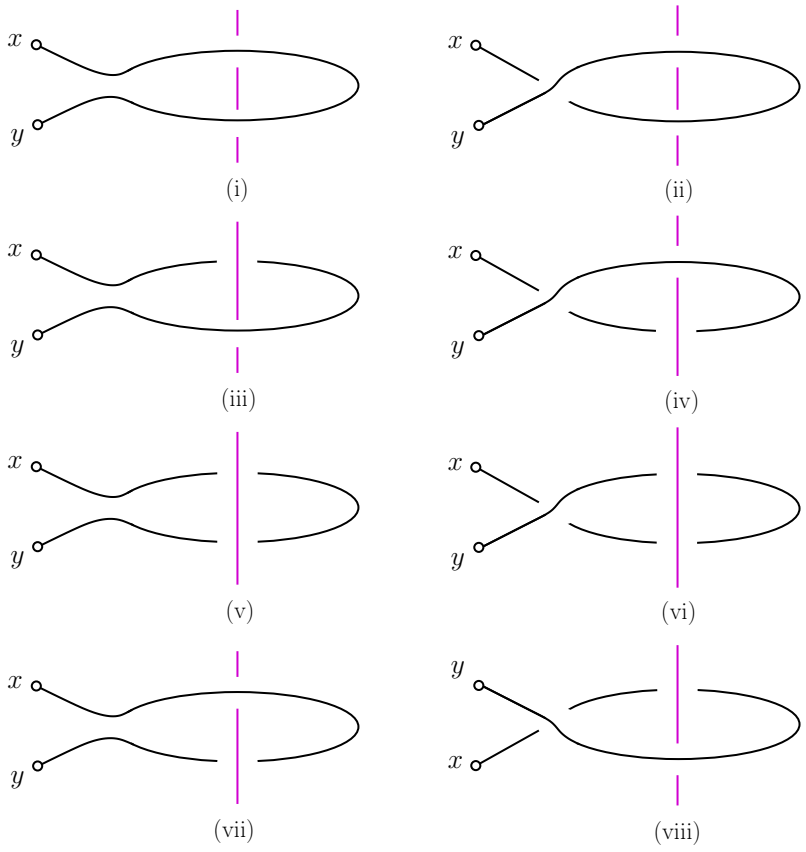

Figure 3.5: Verification of (R3) for the operation of simplifying a Θ [3].

Chapter 4

Characterization of Irreducible Projections

This chapter is dedicated to identifying the structure of irreducible projections. We establish several necessary properties of these projections and ultimately prove that, up to equivalence, only two such projections exist.

4.1 The Central Proposition

The proof of Theorem 1.1 [3] relies crucially on the following foundational proposition:

Proposition 4.1. *[3] Up to equivalence, the set of irreducible projections is completely characterized by the two configurations, P_1 and P_2, depicted in Figure 4.1.*

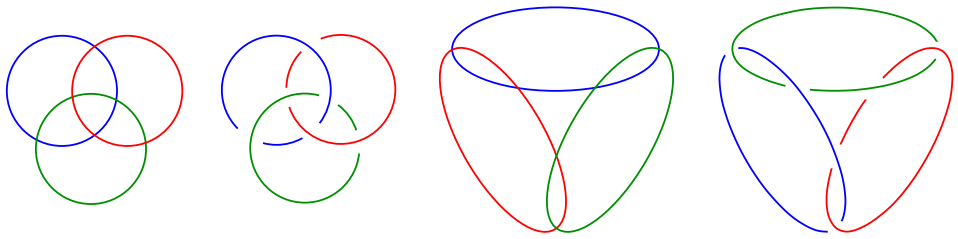

Figure 4.1: The two irreducible projections P_1 and P_2, along with resolutions demonstrating they are projections of $L6n1$.

The remainder of this chapter is committed to proving Proposition 4.1. We begin by analyzing structures that cannot exist within an irreducible projection.

4.2 Forbidden Structures in Irreducible Projections

4.2.1 Disposable Digons

Definition 4.2. ([3]) Let P be a projection. If there exist parallel edges e_1, e_2 such that $e_1 \cup e_2$ bounds an open disk Δ containing no other part of P, then $e_1 \cup e_2$ is called a *digon*. See Figure 4.2.

Let u and v denote the shared endpoints of the edges e_1 and e_2. If e_1 and e_2 belong to the same color class, then both u and v are necessarily monochromatic of that specific color. Conversely, if the edges differ in color, it follows that u and v are bichromatic vertices of the exact same type.

Definition 4.3. ([3]) We define a digon, denoted by $e_1 \cup e_2$, to be *disposable* if it satisfies one of two criteria: either (i) its endpoints u and v are monochromatic; or (ii) u and v are bichromatic, but they do not constitute the unique pair of bichromatic vertices of that specific type within the projection P.

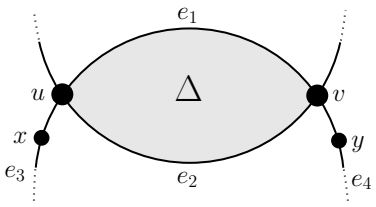

Figure 4.2: A digon. If the digon is disposable, P can be shortcut at x and y.

Observation 4.4. *([3]) It follows naturally that an irreducible projection admits no disposable digons.*

Proof. Assume $e_1 \cup e_2$ is a disposable digon in P. Let e_3 and e_4 be the edges preceding and succeeding e_1 in its straight-ahead walk (Figure 4.2). Subdivide e_3 with x and e_4 with y. The vertices x and y are incident to a common face. Observe that one of the resulting xy-walks traverses exclusively through u and v. Given that the digon is disposable, it strictly follows that the complementary xy-walk must be colourful. Consequently, this configuration permits us to shortcut P at x and y, yielding a reduction that directly contradicts the assumed irreducibility of P. □

4.2.2 Superfluous Walks

Suppose the projection P features a monochromatic vertex v (which, without loss of generality, we assume to be blue). Under this condition, the complete blue walk B decomposes into an edge-disjoint union of two straight-ahead closed walks, denoted β_1 and β_2, both of which are based at v. We formally define these components as the *v-walks*.

Definition 4.5. ([3]) If the walk β_1 satisfies the condition of being colourful, that is, it incorporates at least one blue-red and one blue-green vertex, then the complementary walk β_2 is designated as *superfluous*.

Observation 4.6. *([3]) It naturally follows that an irreducible projection admits no* superfluous *walks.*

Proof. Suppose β_2 is superfluous, meaning β_1 is colourful. Let e_1, e_2 be the edges incident to v belonging to β_2 (Figure 4.3). Subdivide e_1 with x and e_2 with y. One of the resulting xy-walks completely encompasses the edges and vertices of β_1. Because β_1 is inherently colourful, it follows that this enveloping xy-walk must also be colourful. This configuration permits a shortcutting of P at x and y, which establishes a direct contradiction to the assumption that P is irreducible. □

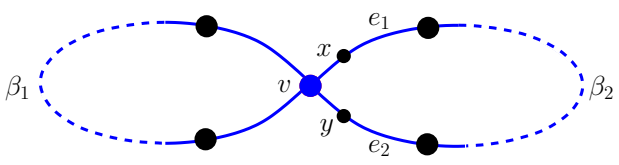

Figure 4.3: Illustration for the proof of Observation 4.6.

4.2.3 Facial Structure

Observation 4.7. *([3]) Within an irreducible projection P, the boundary of every face is strictly a cycle.*

Proof. We demonstrate that the projection P admits no cut vertices—that is, there exists no vertex v for which $P\backslash\{v\}$ is disconnected. Consequently, P is strictly 2-connected, guaranteeing that within its spherical embedding, the boundary of every face constitutes a cycle. Suppose P has a cut vertex v. Such a vertex must be monochromatic (say, blue). Let β_1, β_2 be the v-walks. Because P is a pairwise crossing projection, the red walk R and green walk G necessarily intersect. Suppose, for the sake of contradiction, that v is a cut-vertex. This assumption implies that removing v disconnects the projection. Consequently, to prevent R and G from being topologically separated into disjoint components (which would violate the pairwise crossing property), one of the v-walks, let us assume β_1 must absorb all blue-red and blue-green vertices. This forces β_1 to be colourful, which strictly renders β_2 *superfluous*. However, by Observation 4.6, the existence of a superfluous walk directly contradicts the premise that P is irreducible. □

4.3 Good Sections

The formal introduction of a *good section* serves as an indispensable prerequisite for establishing the proof of Proposition 4.1.

Definition 4.8. ([3]) We define a cycle within the projection P to be *facial* provided that it strictly bounds a face. Furthermore, a *section* of a given facial cycle C is formally defined as a maximal path embedded within C that consists entirely of identically colored edges.

By virtue of the maximality condition defining a section, it strictly follows that its bounding endpoints must be bichromatic vertices.

Definition 4.9. ([3]) A section S is a *good* section if its endpoints are of different types.

For example, a good blue section has one blue-red endpoint, one blue-green endpoint, and any internal vertices are monochromatic blue. We define the *length* of a section as its total number of constituent edges, which may be as few as one [3].

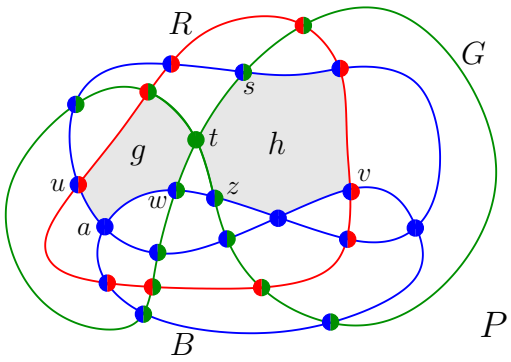

Figure 4.4: As illustrated, the blue path uaw, which constitutes a *good section* of the facial cycle bounding face g, as its endpoints (u and w) are distinctly bichromatic (blue-red and blue-green, respectively). In contrast, the green path stz along the facial cycle bounding face h fails to qualify as a good section, given that both of its endpoints, s and z, share the identical green-blue color pairing.

Observation 4.10. *([3]) Any pairwise crossing projection necessarily admits a minimum of two* good sections *of each respective colour.*

Proof. Consider the decomposition $P = B \cup R \cup G$. Our objective is to demonstrate that P contains a minimum of two good blue sections. To facilitate this, we construct a subgraph P' by deleting all purely green edges and monochromatic green vertices from P, while explicitly preserving the bichromatic green-blue and green-red vertices (as illustrated in Figure 4.5(i)).

Given the pairwise crossing nature of P, the subgraph P' must necessarily contain a face f whose boundary walk W traverses at least one green-blue and one green-red vertex. Consequently, W comprises both blue and red edges, permitting its formal decomposition into an alternating sequence of concatenated sub-walks $W = W_1W_2 \cdots W_k$ (for some even integer k). In this sequence, as illustrated in Figure 4.5(ii), odd indices strictly designate blue walks, while even indices correspond to red walks.

Since W has a blue-green vertex, at least one blue walk (say W_1) contains it. W_1 starts and ends at blue-red vertices (u and v), with internal vertices being blue or blue-green. Let w (resp. z) be the first (resp. last) blue-green vertex encountered traversing W_1 from u to v.

Consequently, the contiguous subwalk extending from u (which is blue-red) to w (blue-green) constitutes a *good section* of a face g within P, as depicted in Figure 4.5(iii). By symmetric reasoning, the subwalk connecting z (blue-green) to v (blue-red) forms a *good section* of another face h in P (Figure 4.5(iv)). This confirms the existence of at least two good blue sections within the projection P. □

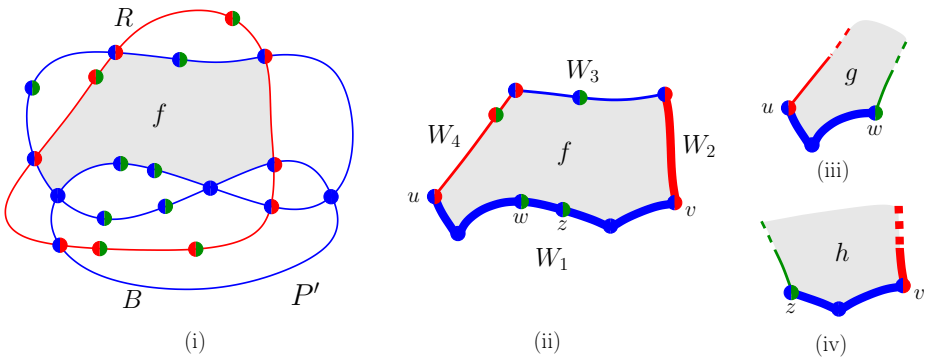

Figure 4.5: Illustration for the proof of Observation 4.10.

4.4 Proof of Proposition 4.1

The proof relies on two main lemmas concerning the length of good sections and the total number of vertices in an irreducible projection.

Lemma 4.11. *([3]) If a projection P is assumed to be irreducible, it necessarily follows that all of its* good sections *must be of length one.*

Lemma 4.12. *([3]) Let P be an irreducible projection wherein every good section has a length of one; it necessarily follows that P comprises exactly six vertices.*

Proof of Proposition 4.1 (assuming Lemmas 4.11 and 4.12). Let $P = B \cup R \cup G$ be an irreducible projection. The aforementioned lemmas restrict P to containing precisely six vertices. Because any pairwise crossing projection necessitates a minimum of two bichromatic vertices for every color pairing, it strictly follows that P is composed of exactly two blue-red, two blue-green, and two red-green vertices, completely devoid of monochromatic vertices. Consequently,

the individual walks B, R, and G must constitute simple cycles that pairwise intersect at exactly two distinct vertices. It is known that any arrangement of three pseudocircles pairwise crossing exactly twice is equivalent to either the Krupp arrangement (P_1) or the non-Krupp arrangement (P_2) (see [12]). Therefore, P is equivalent to P_1 or P_2. □

4.4.1 Proof of Lemma 4.11

Lemma 4.11 follows directly from the subsequent two claims.

Claim 4.13. *([3]) If a projection is irreducible, it inherently follows that no* good section *within it can attain a length of three or more edges.*

Proof. Suppose, for the sake of contradiction, that P contains a good blue section $S = v_0e_1v_1 \dots e_kv_k$ of length $k \geqslant 3$, where v_0 is blue-red and v_k is blue-green (see Figure 4.6). We subdivide the edges e_1, e_2, and e_k with new vertices x, y, and z, respectively. We will demonstrate that at least one vertex pair from $\{(x, y), (x, z), (y, z)\}$ bounds a colourful walk; this permits a shortcut operation, directly violating the irreducibility of P. We traverse the blue walk B originating from x in the direction of v_1 and consider three exhaustive cases: Case 1: y is encountered before v_k. The traversed xy-walk avoids both v_0 and v_k. Consequently, the complementary xy-walk must capture both endpoints, rendering it inherently colourful. Case 2: z is encountered before v_k. By identical logic, the traversed xz-walk avoids v_0 and v_k, forcing the complementary xz-walk to be colourful. Case 3: v_k is encountered first, followed by y and z. The specific segment of the traversal connecting y to z forms a yz-walk devoid of v_0 and v_k. Thus, the alternate yz-walk contains both endpoints and is strictly colourful. □

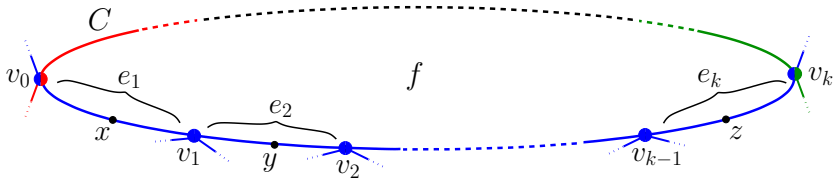

Figure 4.6: Illustration for the proof of Claim 4.13.

Claim 4.14. *([3]) If a projection is assumed to be irreducible, it necessarily follows that no* good section *within it can have a length of precisely two edges.*

Proof. Assume, for the sake of contradiction, that P contains a good blue section $S = ueve'w$ of length exactly two, bounded by a blue-red vertex u and a blue-green vertex w (as illustrated in Figure 4.7). Let B_1 denote the v-walk encompassing u and e, and let B_2 denote the v-walk containing w and e'. Operating under the assumption that P is irreducible, we systematically derive a sequence of structural properties, designated (I) through (V). Ultimately, these properties force the existence of a Θ configuration, providing a direct contradiction to the irreducibility of P.

(I) ([3]) *B_1 contains no blue-green vertex, and B_2 contains no blue-red vertex.*

Proof. If B_1 contained a blue-green vertex, since it also contains u (blue-red), B_1 would be colourful. This makes B_2 superfluous, contradicting Observation 4.6. Similarly for B_2. □

(II) ([3]) *B_1 and B_2 are cycles.*

Proof. Suppose, toward a contradiction, that B_2 is not a cycle. This implies the existence of a blue vertex z within B_2 where all four incident edges are contained within B_2 (Figure 4.8). By

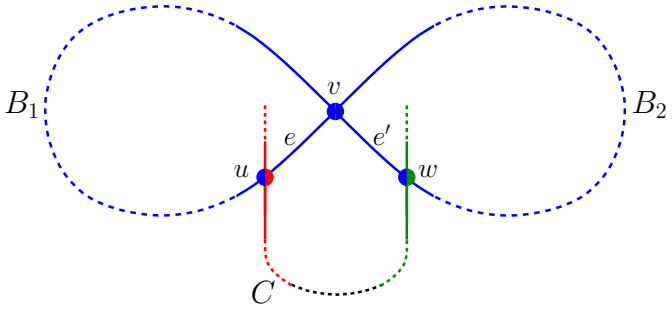

Figure 4.7: Illustration for the proof of Claim 4.14.

construction, the z-walk that contains v must also encompass u and w, rendering it colourful. Consequently, the remaining z-walk is necessarily *superfluous*, which stands in direct contradiction to Observation 4.6. The proof for B_1 follows by symmetry. □

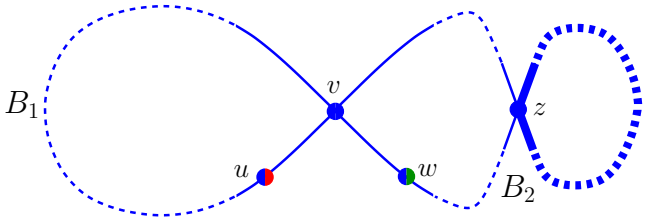

Figure 4.8: Illustration for the proof of (II) in Claim 4.14.

Given that B_2 is a cycle, $\mathbb{S}^2 \backslash B_2$ has two components. Let Δ be the component not containing the blue-red vertex u (shaded region in Figure 4.9).

(III) ([3]) *If $g = st$ is an edge of P contained within Δ having endpoints s and t on B_2, then necessarily $s = w$ or $t = w$.*

Proof. Assume, for the sake of contradiction, that both $s \neq w$ and $t \neq w$ (Figure 4.9). We perform a subdivision on an edge of B_2 incident to s using a new vertex x, and similarly subdivide an edge incident to t using y. Because the edge g connects s and t, the vertices x and y strictly belong to the same face. Consequently, one resulting xy-walk is entirely confined within B_2, while the complementary xy-walk necessarily traverses both u and w. This traversal forces the latter walk to be colourful, thereby permitting a shortcut of P at x and y and directly contradicting its assumed irreducibility. □

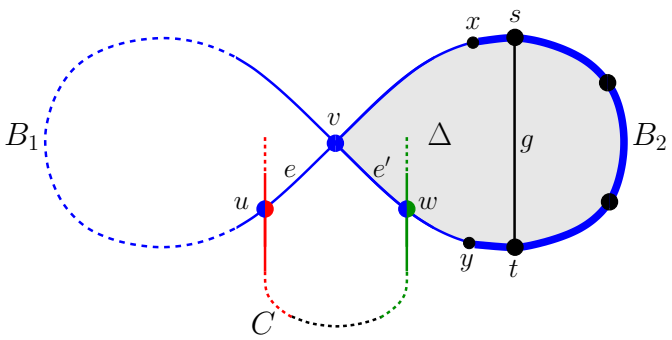

Figure 4.9: Illustration for the proof of (III) in Claim 4.14.

(IV) ([3]) *The vertex v is the strictly unique blue vertex.*

Proof. Suppose, for the sake of contradiction, that there exists an additional blue vertex $s \neq v$. Because B_1 and B_2 are established as cycles, it follows that $s \in B_1 \cap B_2$. Consequently, there must exist a subpath Q of B_1 traversing the interior of Δ, originating at s and terminating at some vertex t (Figure 4.10). By Property (III), Q cannot consist of a single edge; therefore, it must contain at least one internal vertex, z. Because all blue vertices are strictly confined to the boundary of Δ, z cannot be blue. Furthermore, if z were blue-green, the cycle B_1 (which already contains the blue-red vertex u) would become colourful, rendering B_2 superfluous. We are thus forced to conclude that z is blue-red.Examining the walks emanating from t, we observe that one specific t-walk encompasses w, v, s, and z. Given that w is blue-green and z is blue-red, this particular t-walk is inherently colourful. This immediately renders the complementary t-walk superfluous, yielding a direct contradiction. □

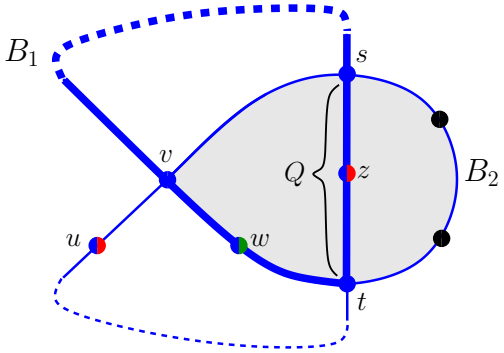

Figure 4.10: Illustration for the proof of (IV) in Claim 4.14.

(V) ([3]) *The interior of* Δ *contains no green vertices.*

Proof. Assume, for the sake of contradiction, that a green vertex z resides strictly within Δ. Under this assumption, the red walk R must be entirely restricted to the exterior of Δ. Were R to enter Δ, it would necessarily intersect the boundary B_2, which implies the existence of a blue-red vertex on B_2; this directly contradicts Property (I). Now consider G_1 and G_2, the two green walks emanating from z. By definition, at least one of these walks, say G_1, must contain a green-red vertex. Because R lies strictly outside Δ and z lies strictly inside, the path of G_1 is forced to cross the boundary B_2. This crossing dictates that G_1 captures a green-blue vertex, thereby making G_1 colourful. Consequently, G_2 is rendered superfluous, which establishes our contradiction. □

Finale of the proof of Claim 4.14 ([3]). We assert that the interior of Δ is strictly devoid of any vertices. To verify this, suppose a vertex z lies within Δ. Since the red walk R is strictly exterior to Δ, z can be neither red nor red-bichromatic. By Property (IV), v is the unique blue vertex, precluding any blue edges from entering Δ and ensuring z is neither blue nor blue-bichromatic. Furthermore, Property (V) dictates that z cannot be green. Consequently, Δ contains zero vertices.

Let e_w denote the green edge incident to w that traverses the interior of Δ. Because Δ contains no internal vertices, the opposite endpoint of e_w is forced to be a blue-green vertex q residing on B_2 (Figure 4.11). We claim e_w constitutes the entirety of P within Δ. If an additional edge $g = st$ existed inside Δ, its endpoints s and t would necessarily lie on B_2. Given $g \neq e_w$, neither s nor t can be w, which directly violates Property (III).

It follows that e_w is the sole element of P occupying Δ. This geometric constraint restricts the vertices of B_2 to exactly v, q, and w. Therefore, the union $B_2 \cup \{e_w\}$ inevitably forms a Θ in P, establishing a fatal contradiction to the assumed irreducibility of P. □

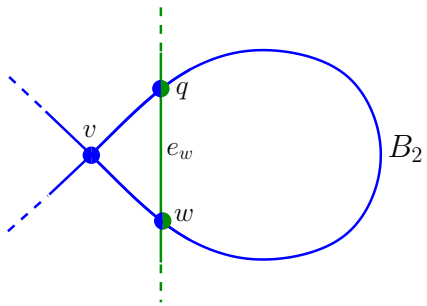

Figure 4.11: Conclusion of the proof of Claim 4.14.

4.4.2 Proof of Lemma 4.12

We are now in a position to establish Lemma 4.12, utilizing the aforementioned properties in conjunction with Euler's formula.

Proof of Lemma 4.12. Let P be an irreducible projection constrained such that all of its good sections possess a length of exactly one, forming what we will call *good edges*. From Observation 4.10, we deduce that such a projection P necessarily admits at least two good edges of each color. □

Claim A. ([3]) *There exist no monochromatic vertices within the projection P.*

Proof. Assume, for the sake of contradiction, that P contains a monochromatic blue vertex u. Consider an arbitrary good blue edge e. The topology of P dictates that one of the two walks originating from u must traverse e, thereby encompassing both its blue-red and blue-green endpoints. This inclusion strictly renders the traversed u-walk colourful. Consequently, the complementary u-walk is reduced to being superfluous, which constitutes a direct violation of Observation 4.6. □

For any given face f in P, its degree $|f|$ *is defined as the number of edges that constitute its boundary walk.*

Claim B. *([3]) If the projection P possesses three or more faces of degree two, then the total vertex count of P is strictly constrained to exactly six.*

Proof. Suppose P has three faces f_1, f_2, f_3 of degree 2, bounded by digons D_1, D_2, D_3. By Claim A (no monochromatic vertices), the vertices of each digon are bichromatic of the same type. Assume vertices of D_1 are blue-red. By Observation 4.4, these must be the only blue-red vertices in P (otherwise D_1 is disposable). Assume vertices of D_2 are blue-green. Similarly, it follows that no other blue-green vertices exist within P. The vertices of D_3 must then be red-green, and they are the only ones. Since all vertices are bichromatic (Claim A), P has exactly six vertices. □

Claim C. *([3]) The projection P possesses a maximum of three faces having a degree of four or greater.*

Proof. Assume, toward a contradiction, that P contains four or more faces with a degree of at least four. Because the projection utilizes only three colors, any facial boundary containing four or more edges must, by the Pigeonhole Principle, contain at least two edges of the same color. Applying the Pigeonhole Principle a second time to these four faces reveals that there must exist a specific color—without loss of generality, let us say blue—such that two distinct faces, f and f', each contain at least two blue edges in their respective boundaries. Let these blue edges be e_1 and e_2 on the boundary of f, and e_3 and e_4 on the boundary of f'.We know P possesses at least two good blue edges.

Consequently, there must exist a good blue edge e that is disjoint from either the set $\{e_1, e_2\}$ or the set $\{e_3, e_4\}$. Let us assume the former: $e \notin \{e_1, e_2\}$. We subdivide e_1 with a new vertex x, and e_2 with a new vertex y. Because e_1 and e_2 border the same face f, x and y are co-facial. Tracing the boundary, one of the resulting xy-walks must traverse the good edge e. Given that e is bounded by a blue-red and a blue-green vertex, this specific xy-walk is strictly colourful. This configuration permits a shortcut operation across f between x and y, yielding a direct contradiction to the irreducibility of P. □

Conclusion of the proof of Lemma 4.12

Proof. According to Claim A, P contains no monochromatic vertices. This absence implies that the walks B, R, and G must necessarily be cycles. Since any two of these cycles intersect in an even number of vertices, it naturally follows that the total number of vertices in P is even. We show P cannot have $n \geqslant 8$ vertices.

Assume that $n \geqslant 8$. Given that the projection P is exactly 4-regular, it consequently contains $2n$ edges. A direct application of Euler's formula establishes that P comprises $n + 2$ faces. Let these faces be denoted by $f_1, \ldots, f_{n+2}$, indexed such that their degrees are ordered. By the fundamental property of planar graphs, the sum of all face degrees must equal twice the total number of edges, yielding the equation $\sum_{i=1}^{n+2} |f_i| = 4n$

By Claim B, for $n \geqslant 8$, P possesses a maximum of two faces of degree two, implying $|f_3| \geqslant 3$. Concurrently, Claim C restricts P to at most three faces of degree four or greater, dictating $|f_{n-1}| \leqslant 3$. These bounds strictly force $|f_3| = |f_4| = \cdots = |f_{n-1}| = 3$, yielding exactly $n-3$ faces of degree three. Given $n \geqslant 8$, P contains no fewer than five triangular faces. Because P lacks monochromatic vertices (Claim A), every degree-three face must be bounded by a cycle comprising one blue, one red, and one green edge, which inherently makes them good edges. With at least five such faces, and each edge being incident to exactly two faces, a simple counting argument guarantees the existence of at least three good edges per color class.

We now assert that this condition strictly prohibits the existence of any face with a degree of four or greater. Assume, toward a contradiction, that a face f has degree $|f| \geqslant 4$. By the Pigeonhole Principle, its boundary contains two edges, e' and e'', of identical color (assume blue). Since we established the presence of at least three good blue edges, there exists a good blue edge $e \notin \{e', e''\}$. Subdividing e' at x and e'' at y creates an xy-walk containing e. Because e is a good edge, this walk is inherently colourful, permitting a shortcut of P across f and directly contradicting irreducibility.

Therefore, all faces have degree at most 3. So $|f_n| = |f_{n+1}| = |f_{n+2}| = 3$. We estimate the sum of degrees: $\sum_{i=1}^{n+2} |f_i| = |f_1| + |f_2| + \sum_{i=3}^{n+2} |f_i| \leqslant 3 + 3 + 3n = 3n + 6$. Since the sum must equal $4n$, we have $4n \leqslant 3n + 6$, which implies $n \leqslant 6$. This contradicts the assumption $n \geqslant 8$. Thus, P must have exactly six vertices. □

Chapter 5

Main Theorem and Applications

Having characterized the irreducible projections, we can now demonstrate the main theorem of this thesis and explore some of its consequences regarding the Taniyama relation.

5.1 Proof of the Main Theorem

We restate the main theorem and provide its proof using the results established in the previous chapters.

Theorem 5.1. *([3]) A projection of a* 3*-component link constitutes a projection of the link* $L6n1$ *if and only if it is pairwise crossing.*

Proof of Theorem 5.1. The "only if" direction is straightforward. The link $L6n1$ is pairwise linked (its components cannot be separated). Therefore, any projection of $L6n1$ must necessarily be pairwise crossing.

We now establish the sufficiency condition: every projection exhibiting the pairwise crossing property is strictly a projection of the link $L6n1$. Let P denote a fixed pairwise crossing projection. Our objective is to rigorously demonstrate that $L6n1 \in \textsc{Link}(P)$

Given P, we can iteratively apply the reduction operations (shortcutting and simplifying a Θ). Due to properties (R1) (fewer vertices) and (R2) (preserves pairwise crossing), this process terminates at an irreducible projection P'. Due to property (R3) ($\textsc{Link}(\overline{P}) \subseteq \textsc{Link}(P)$), an iterative application yields $\textsc{Link}(P') \subseteq \textsc{Link}(P)$.

Proposition 4.1 dictates that the only possible irreducible projections are P_1 and P_2. This yields the property (†): either $\textsc{Link}(P_1) \subseteq \textsc{Link}(P)$ or $\textsc{Link}(P_2) \subseteq \textsc{Link}(P)$.

Recall from Figure 4.1 that resolving either P_1 or P_2 can yield the link $L6n1$, establishing that $L6n1 \in \textsc{Link}(P_1)$ and $L6n1 \in \textsc{Link}(P_2)$. Combined with (†), this guarantees that $L6n1 \in \textsc{Link}(P)$. □

5.2 Applications to the Taniyama Relation

Taniyama investigated a relation $\geqslant$ on links in [32].

Definition 5.2. ([3]) For two given links L_1 and L_2, we define the relation $L_1 \geqslant L_2$ to hold if and only if every valid projection of L_1 also serves as a projection of L_2. Under this condition, L_2 is termed a *minor* of L_1, and conversely, L_1 is said to *majorize* L_2.

Applying Theorem 5.1, we proceed to systematically characterize both the links that majorize $L6n1$ and those that emerge as its minors. Throughout this discussion, our domain of discourse is strictly restricted to three-component links.

5.2.1 Links Majorizing $L6n1$

Observation 5.3. *([3]) We establish that a link majorizes $L6n1$ if and only if its constituent components are strictly pairwise linked.*

The foundation of the forthcoming proof rests firmly upon an established topological result regarding the realization of sublink diagrams.

Theorem 5.4 (Lee and Jin, [23])**.** *Let L be a link partitioned into a collection of sublinks $L_1, \ldots, L_n$, where each sublink L_i admits a corresponding diagram D_i. Under these conditions, there exists a comprehensive diagram D of the entire link L such that the restriction of D to any given sublink L_i is isotopic to its respective diagram D_i.*

An immediate consequence is:

Corollary 5.5. *([3]) Let L denote a link whose components fail to be universally pairwise linked. Under such conditions, there inherently exists a diagram D of L wherein at least two distinct components exhibit absolutely no mutual crossings.*

Proof of Observation 5.3. Sufficiency : Assume that the components of L are pairwise linked. It follows topologically that every projection of L must be pairwise crossing. By Theorem 5.1, this guarantees that every projection of L is inherently a projection of $L6n1$. Consequently, by definition, L majorizes $L6n1$.

Necessity : Conversely, suppose that the components of L are not pairwise linked. By Corollary 5.5, there exists at least one projection P of L that fails to be pairwise crossing. According to Theorem 5.1, this specific projection P cannot be a projection of $L6n1$. Because L possesses a projection not belonging to $L6n1$, it definitively does not majorize $L6n1$. □

5.2.2 Minors of $L6n1$

We now proceed to fully characterize the set of links that emerge as minors of $L6n1$. Excluding $L6n1$ itself, this collection consists of the three distinct links depicted in Figure 5.1. To formally encapsulate this family, we define the set $\mathcal{L}$ as follows:

$$\mathcal{L} := \{0_1 \cup 0_1 \cup 0_1, 0_1 \cup L2a1, L2a1\#L2a1, L6n1\}.$$

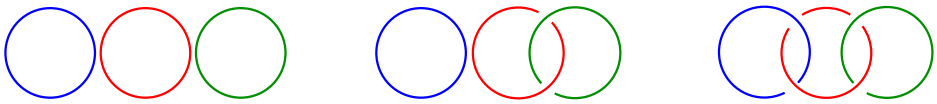

$0_1 \cup 0_1 \cup 0_1$ $\quad$ $0_1 \cup L2a1$ $\quad$ $L2a1\#L2a1$

Figure 5.1: Links that are minors of $L6n1$ (excluding $L6n1$ itself).

Observation 5.6. *([3]) We can notice that a link L constitutes a minor of $L6n1$ if and only if $L \in \mathscr{L}$.*

The proof utilizes the specific resolution possibilities of the irreducible projections P_1 and P_2. The following facts can be verified by analyzing all possible resolutions of P_1 and P_2.

Remark 5.7. ([3]) The projection P_1 admits exactly five distinct link resolutions: the four constituent links comprising the set $\mathscr{L}$ alongside the link $L6a4$, commonly recognized as the Borromean rings. Formally, this establishes the identity $\textsc{Link}(P_1) = \mathcal{L} \cup \{L6a4\}$.

Remark 5.8. ([3]) The projection P_2 admits exactly five distinct link resolutions: the four constituent links within $\mathscr{L}$ and the link $L6a5$. This exhaustiveness is captured by the identity $\textsc{Link}(P_2) = \mathcal{L} \cup \{L6a5\}$.

Proof of Observation 5.6. Sufficiency: Suppose L is a minor of $L6n1$. By definition, any projection of $L6n1$ must also serve as a projection of L. Given that P_1 and P_2 are projections of $L6n1$, they are necessarily projections of L, implying $L \in \textsc{Link}(P_1)$ and $L \in \textsc{Link}(P_2)$. Invoking Remarks 5.7 and 5.8, we observe that L must reside in the intersection of these resolution sets: $L \in \textsc{Link}(P_1) \cap \textsc{Link}(P_2) = \mathcal{L}$.

Necessity: Conversely, let $L \in \mathcal{L}$. To establish that L is a minor of $L6n1$, we must demonstrate that every projection of $L6n1$ is a projection of L. By Theorem 5.1, it suffices to show that any arbitrary pairwise crossing projection P is a projection of L. Recall from the proof of Theorem 5.1 that P being pairwise crossing implies either $\textsc{Link}(P_1) \subseteq \textsc{Link}(P)$ or $\textsc{Link}(P_2) \subseteq \textsc{Link}(P)$. Since $\mathcal{L}$ is a subset of both $\textsc{Link}(P_1)$ and $\textsc{Link}(P_2)$ (per Remarks 5.7 and 5.8), it follows that $\mathcal{L} \subseteq \textsc{Link}(P)$ in either case. Given $L \in \mathcal{L}$, we conclude $L \in \textsc{Link}(P)$, confirming that P is indeed a projection of L. □

Part III

Positive Links and Arrangements of Pseudocircles

Chapter 6

Ring Links

For brevity, we designate any link belonging to the set $\overrightarrow{\mathcal{L}}^{+}(\mathscr{R}_n)$ as a *positive ring link of size* n, or more concisely, a *ring link of size* n. This nomenclature is adopted with the understanding that all links under consideration in this section are assumed to be positive [27].

6.1 Correspondence Between Ring Links and Binary Words

A ring link of size n possesses a natural correspondence with a binary word of length n [27]. Each element of $\overrightarrow{\mathcal{L}}^{+}(\mathscr{R}_n)$ is constructed by prescribing an orientation to each of the n constituent pseudocircles within $\mathscr{R}_n$. This orientational assignment is systematically encoded as a binary sequence, following the convention illustrated in Figure 6.1.

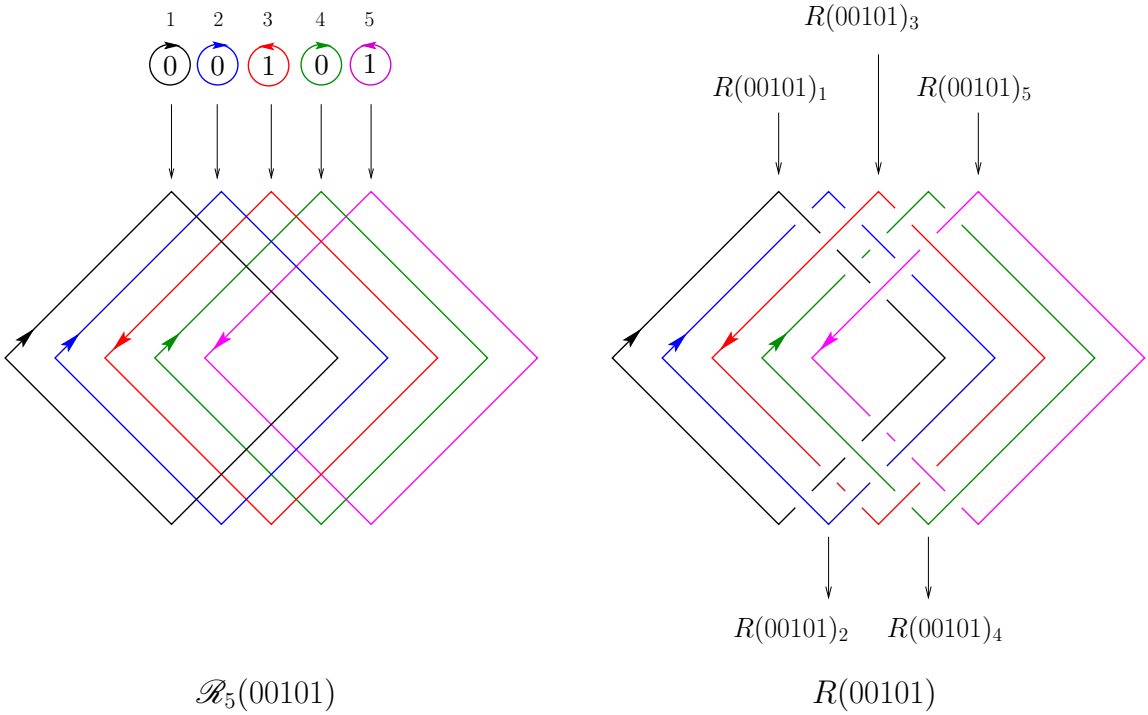

Figure 6.1: The oriented arrangement $\mathscr{R}_5(00101)$ yields a corresponding positive link, the ring link $R(00101)$. For this link, we label the five individual components as $R(00101)_1, R(00101)_2, R(00101)_3, R(00101)_4$, and $R(00101)_5$.

Let the pseudocircles in $\mathscr{R}_n$ be indexed $i \in \{1, \ldots, n\}$, ordered strictly from left to right. We encode the orientation of the arrangement using a binary word a of length n, where the i-th entry

is defined as 0 if pseudocircle i is oriented clockwise and 1 if it is oriented counter-clockwise [27]. We denote the resulting oriented arrangement by $\mathscr{R}_n(a)$ and its induced positive link by $R(a)$.

For an illustration, in $\mathscr{R}_5$, orienting pseudocircles $1, 2, 4$ clockwise and $3, 5$ counterclockwise yields the oriented arrangement $\mathscr{R}_5(00101)$ (Figure 6.1, left), inducing the ring link $R(00101)$ (Figure 6.1, right). The i-th component of $R(a)$ is denoted $R(a)_i$.

In summary, we establish a formal bijection between the set of binary words of length n and the collection $\overrightarrow{\mathcal{L}}^+(\mathscr{R}_n)$ of ring links of size n [27]. This bijective correspondence extends naturally to both boot links and flower links. For the remainder of this text, we shall refer to a binary word simply as a *word*.

We now establish the requisite terminology for word operations as in [27]. For a word $a = a_1 \cdots a_n$, we define its *reverse*, denoted a^{-1}, as the sequence $a_n \cdots a_1$. Furthermore, its *negation* $\overline{a}$ is given by $\overline{a_1} \cdots \overline{a_n}$, where we adopt the convention $\overline{0} = 1$ and $\overline{1} = 0$. We observe that these operations commute, yielding the identity $(\overline{a})^{-1} = \overline{a^{-1}}$.

We define a *subword* [27] of a as any sequence $a_{i_1} \cdots a_{i_m}$ such that the indices satisfy $1 \leqslant i_1 < \cdots < i_m \leqslant n$. Furthermore, a word is said to be *oscillating* [27] if it contains no consecutive identical bits (i.e., it avoids the patterns 00 and 11). We adopt the term 'oscillating' specifically to preclude any confusion with the standard notion of alternating links in knot theory.

A word is said to be *monotone* [27] if it is composed entirely of 0s or entirely of 1s. We measure the complexity of a word a via its *rank* [27], $\mathrm{rank}(a)$, which is the length of its longest oscillating subword. As an example, $\mathrm{rank}(001100) = 3$ because the longest subword avoiding consecutive identical bits is of length three.

We employ the notation 0^m and 1^m to denote the monotone words consisting of m zeros and m ones, respectively.

If $a_{i_1} \cdots a_{i_r}$ represents a maximal oscillating subword of a, it follows that a can be partitioned into a concatenation of r monotone blocks: $a = A_1 \cdots A_r$, where each block A_j consists of the bit a_{i_j} repeated $\alpha(j)$ times. We refer to these blocks A_j as the *canonical subwords* [27] of a, and the resulting expression as its *canonical decomposition* [27]. This structure is exemplified in Figure 6.2

$$\overbrace{\underbrace{00}_{A_1}\ \underbrace{1}_{A_2}\ \underbrace{000}_{A_3}\ \underbrace{11}_{A_4}\ \underbrace{0}_{A_5}}^{a\,=\,001000110}$$

Figure 6.2: As an illustration, consider the word $a = 0010001100$. Its canonical decomposition is given by $a = A_1A_2A_3A_4A_5$, where the canonical subwords are defined as $A_1 = 0^2, A_2 = 1^1, A_3 = 0^3, A_4 = 1^2$, and $A_5 = 0^2$.

6.2 Isotopies Acting Naturally on Ring Links

The proof of Theorem 1.2 centers on identifying which ring links are equivalent to $R(a)$. The easy part is showing that $R(a)$ is always equivalent to $R(\overline{a})$, $R(a^{-1})$, and $R((\overline{a})^{-1})$ (Observation 6.1). The difficult part is proving these are the *only* equivalent links (Proposition 6.2).

We first show $R(a) \sim R(\overline{a})$. Consider the isotopy $\mathcal{H}$ (for "horizontal"), a 180-degree rotation around a horizontal axis in the plane of the diagram (Figure 6.3). Applying $\mathcal{H}$ to $R(a)$ results in $R(\overline{a})$. That is, $\mathcal{H} \,\big|\, R(a) \to R(\overline{a})$. Thus, (R1) *for any word* a, $R(a) \sim R(\overline{a})$.

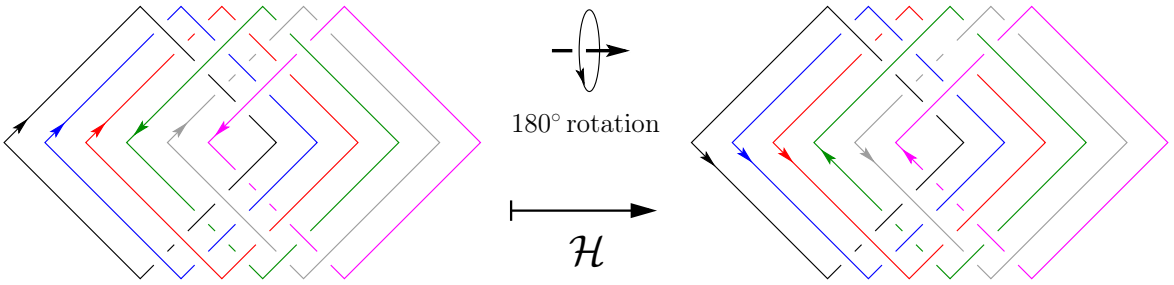

$R(000101)$ $\qquad$ $R(\overline{000101})=R(111010)$

Figure 6.3: If we apply the isotopy $\mathcal{H}$ to the ring link $R(000101)$ we obtain the ring link $R(\overline{000101}) = R(111010)$. The permutation of this $R(000101) \mapsto R(111010)$ isotopy is the identity permutation ι on [6]. In general, $\mathcal{H} \,\big|\, R(a) \xrightarrow{\iota} R(\overline{a})$.

Now consider the isotopy $\mathcal{V}$ (for "vertical"), a 180-degree rotation around a vertical axis in the plane of the diagram (Figure 6.4). Applying $\mathcal{V}$ to $R(a)$ results in $R\big((\overline{a})^{-1}\big)$. That is, $\mathcal{V} \,\big|\, R(a) \to R((\overline{a})^{-1})$. Thus, (R2) *for any word* a, $R(a) \sim R((\overline{a})^{-1})$.

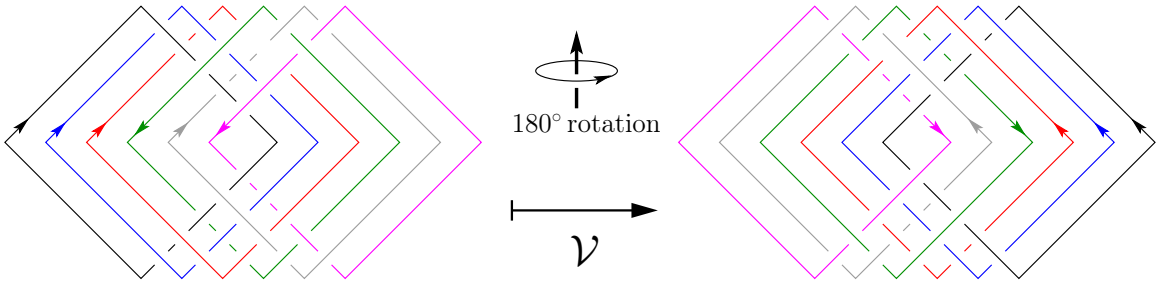

$R(000101)$ $\qquad$ $R\big(\overline{(000101)^{-1}}\big)=R\big((\overline{000101})^{-1}\big)=R(010111)$

Figure 6.4: If we apply the isotopy $\mathcal{V}$ to the ring link $R(000101)$ we obtain the ring link $R((\overline{000101})^{-1}) = R(010111)$. The permutation of this $R(000101) \mapsto R(010111)$ isotopy is the reverse permutation ν on [6]. In general, $\mathcal{V} \,\big|\, R(a) \xrightarrow{\nu} R((\overline{a})^{-1})$.

Applying $\mathcal{H}$ followed by $\mathcal{V}$ (the composition $\mathcal{V} \circ \mathcal{H}$) to $R(a)$ yields $R((\overline{\overline{a}})^{-1}) = R(a^{-1})$. Thus, (R3) *for any word* a, $R(a) \sim R(a^{-1})$.

Trivially, (R4) $R(a) \sim R(a)$. Combining (R1)–(R4) gives:

Observation 6.1. *([27]) Let* a *and* b *be words. If* b *is either* $a, \overline{a}, a^{-1}$, *or* $(\overline{a})^{-1}$, *then* $R(a) \sim R(b)$.

6.3 Reduction of Theorem 1.2

We have identified four words b such that $R(a) \sim R(b)$. The main component in the proof of Theorem 1.2 is the converse statement, provided the rank of a is at least four:

Proposition 6.2. *([27]) Let a be a word of rank $r \geqslant 4$. If b is a word such that $R(a) \sim R(b)$, then b is either $a, \overline{a}, a^{-1}$, or $(\overline{a})^{-1}$.*

We defer the proof of this proposition and first show that Theorem 1.2 follows from it.

Proof of Theorem 1.2 (assuming Proposition 6.2). Let a be a word of length n. Standard calculations show that as $n \to \infty$, the probability that $\mathrm{rank}(a) < 4$ approaches 0. Also, the probability that the set $\{a, \overline{a}, a^{-1}, (\overline{a})^{-1}\}$ contains fewer than four distinct words approaches 0. By Observation 6.1 and Proposition 6.2, the probability that there are *exactly* four distinct words b such that $R(a) \sim R(b)$ converges to 1 as $n \to \infty$.

The established bijection between binary words and the set $\overrightarrow{\mathcal{L}}^{+}(\mathscr{R}_n)$ implies that the proportion of equivalence classes in $\overrightarrow{\mathcal{L}}^{+}(\mathscr{R}_n)$ with a cardinality of exactly four approaches unity as $n \to \infty$. Given that $|\overrightarrow{\mathcal{L}}^{+}(\mathscr{R}_n)| = 2^n$, the asymptotic result stated in Theorem 1.2 follows as a direct consequence. □

6.4 Proof of Proposition 6.2

We now focus on proving Proposition 6.2 by reducing it to two key lemmas. We first discuss sublinks of ring links.

6.4.1 Sublinks of Ring Links

Let $a = a_1 \dots a_n$ be a word, and $1 \leqslant i_1 < \cdots < i_k \leqslant n$. The subword $a_{i_1} \cdots a_{i_k}$ corresponds to the link $R(a)_{i_1} \cup \cdots \cup R(a)_{i_k}$. This is a *sublink* [27] of $R(a)$, denoted $R(a)_{i_1,\dots,i_k}$.

The ring link $R(a)$ (or sublink $R(a)_{i_1,\dots,i_k}$) is *oscillating* if the corresponding word a (or subword $a_{i_1} \cdots a_{i_k}$) is oscillating. The size of an oscillating sublink is bounded by the rank r of a.

6.4.2 Reduction to Two Lemmas

The proof of Proposition 6.2 relies on two main ingredients. The first (Lemma 6.3) states that if $R(a) \sim R(b)$ via an isotopy $\mathcal{I}$, then b can be reconstructed by the action of $\mathcal{I}$ on an oscillating sublink $R(a)_{i_1,\dots,i_r}$ of maximal size r. Specifically, knowing the image subword and the induced permutation determines b.

The second ingredient (Lemma 6.4) characterizes these possibilities: the image subword must also be oscillating, and the induced permutation must be ι or ν.

We use the concept of a π-image,see Figure 6.5. If $a = A_1 \cdots A_r$ and $b = B_1 \cdots B_r$ are canonical decompositions, b is the *π-image* of a if $|A_i| = |B_{\pi(i)}|$ for $i = 1, \dots, r$.

Lemma 6.3. *([27]) Let a be a word with rank $r \geqslant 4$, let b be a word such that $R(a) \sim R(b)$, and let $\mathcal{I}$ be an $R(a) \mapsto R(b)$ isotopy. Let $R(a)_{i_1,\dots,i_r}$ be an oscillating sublink of $R(a)$, and let $R(b)_{j_1,\dots,j_r}$ be its image under $\mathcal{I}$. Then b is the π-image of a, where π is the $(R(a_{i_1,\dots,i_r}), R(b_{j_1,\dots,j_r}))$-permutation under $\mathcal{I}$.*

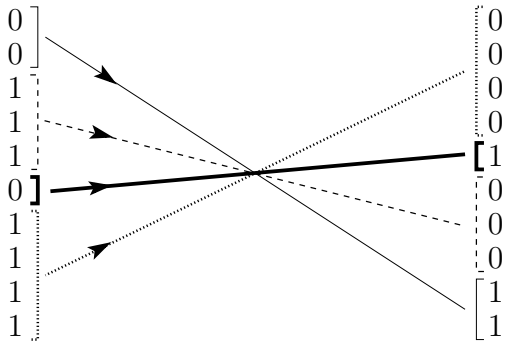

$a = 0011101111 = 0^2 1^3 0^1 1^4 \qquad b = 0000100011 = 0^4 1^1 0^3 1^2$

Figure 6.5: Let $a = 0011101111$ be defined by the canonical decomposition $A_1A_2A_3A_4$, such that $A_1 = 00 = 0^2, A_2 = 111 = 1^3, A_3 = 0 = 0^1$, and $A_4 = 1111 = 1^4$. Similarly, let $b = 0000100011$ be defined by $B_1B_2B_3B_4$, where the components are $B_1 = 0000 = 0^4, B_2 = 1 = 1^1, B_3 = 000 = 0^3$, and $B_4 = 11 = 1^2$. We utilize arrows to depict a natural bijection between the respective canonical subwords. If we take π to be the reverse permutation $\nu = (4\,3\,2\,1)$ on $[4]$, it follows that A_i maps to (and shares the same length as) $B_{\pi(i)}$ for $i = 1, 2, 3, 4$. This relationship establishes b as the π-image of a.

Lemma 6.4. *([27]) Let a be a word of rank $r \geqslant 4$, and $R(a)_{i_1,\ldots,i_r}$ an oscillating sublink of size r. Let $R(a) \sim R(b)$ via isotopy $\mathcal{I}$, and let $R(b)_{j_1,\ldots,j_r}$ be the image of $R(a)_{i_1,\ldots,i_r}$. Then,*

(1) the $(R(a)_{i_1,\ldots,i_r}, R(b)_{j_1,\ldots,j_r})$-permutation under $\mathcal{I}$ is either ι or ν; and

(2) $b_{j_1} \cdots b_{j_r}$ is an oscillating subword of b.

We defer the proofs of these lemmas and first establish Proposition 6.2 assuming they hold. We note a consequence of Lemma 6.4.

Corollary 6.5. *([27]) If a is a word such that rank $r \geqslant 4$. And the ring link $R(a)$ is equivalent to $R(b)$, then it follows that* $\operatorname{rank}(b) = r$.

Proof. Let $s := \operatorname{rank}(b)$. According to Lemma 6.4, the equivalence $R(a) \sim R(b)$ implies that $R(b)$ contains an oscillating sublink of size r, which necessitates $s \geqslant r$. Consequently, we have $\operatorname{rank}(b) \geqslant 4$. By applying the same lemma symmetrically to the isotopy $R(b) \mapsto R(a)$, it follows that $R(a)$ must possess an oscillating sublink of size s, implying $r \geqslant s$. Therefore, we conclude that $s = r$. □

Proof of Proposition 6.2 (assuming Lemmas 6.3 and 6.4). Let a have rank $r \geqslant 4$, and $R(a) \sim R(b)$ via $\mathcal{I}$. Let $R(a)_{i_1,\ldots,i_r}$ be an oscillating sublink, $R(b)_{j_1,\ldots,j_r}$ its image, and π the induced permutation.

Since $a_{i_1} \cdots a_{i_r}$ is oscillating, by Lemma 6.4 (2), $b_{j_1} \cdots b_{j_r}$ is either:

(†) $a_{i_1} \cdots a_{i_r}$; or

(‡) $\overline{a_{i_1} \cdots a_{i_r}}$.

Let $a = A_1 \cdots A_r$ and $b = B_1 \cdots B_r$ be the respective canonical decompositions of a and b, where $\operatorname{rank}(b) = r$ by Corollary 6.5. Lemma 6.3 implies that b is the π-image of a. Since Lemma 6.4,(1) restricts the permutation to $\pi \in \{\iota, \nu\}$, we obtain two possible constraints on the block lengths:

(∗) $|B_k| = |A_k|$ for all k (the case where $\pi = \iota$);

$(**)$ $|B_k| = |A_{r-k+1}|$ for all k (the case where $\pi = \nu$).

By synthesizing these length conditions with the orientation cases, we conclude: If $(*)$ and $(\dagger)$ hold, then $b = a$. If $(*)$ and $(\ddagger)$ hold, then $b = \overline{a}$.If $(**)$ and $(\dagger)$ hold, then $b = a^{-1}$.If $(**)$ and $(\ddagger)$ hold, then $b = (\overline{a})^{-1}$. □

6.5 Proof of Lemma 6.3

We highlight the methodology of this proof because its logic is recurrent; the same structural approach will be employed in later sections for boot and flower links.

Proof of Lemma 6.3 (assuming Lemma 6.4). Given the canonical decomposition $a = A_1 \cdots A_r$, we define the *k-th canonical sublink*, denoted $R_k(a)$, as the set of components corresponding to the monotone block A_k. The full ring link $R(a)$ is thus the union of these disjoint canonical sublinks. Furthermore, a sublink of size r is oscillating if and only if it is formed by selecting exactly one component from each $R_k(a)$.

By Corollary 6.5, $\mathrm{rank}(b) = r$. Let $b = B_1 \cdots B_r$ be its canonical decomposition, and $R_k(b)$ the corresponding canonical sublinks.

The oscillating sublink $R(a)_{i_1,\ldots,i_r}$ has $R(a)_{i_k} \in R_k(a)$. The permutation π means $\mathcal{I}$ maps $R(a)_{i_k}$ to $R(b)_{j_{\pi(k)}}$, which belongs to $R_{\pi(k)}(b)$.

The central argument rests on the following claim:$(\dagger)$ For each $k \in \{1, \ldots, r\}$, the isotopy $\mathcal{I}$ maps every component of $R_k(a)$ to a component in $R_{\pi(k)}(b)$.

To establish $(\dagger)$, suppose for the sake of contradiction that some component $R(a)_{i'_k} \in R_k(a)$ is mapped to a component outside of $R_{\pi(k)}(b)$. Consider an oscillating sublink of $R(a)$ that includes $R(a)_{i_k}$; if we replace $R(a)_{i_k}$ with $R(a)_{i'_k}$, the new sublink remains oscillating. However, its image under $\mathcal{I}$ would then lack any component from $R_{\pi(k)}(b)$, which implies the image is no longer oscillating. This directly contradicts the requirement that $\mathcal{I}$ preserves oscillating sublinks as per Lemma 6.4(2). Thus, $(\dagger)$ must hold.

Since $|R_k(a)| = |A_k|$ and $|R_{\pi(k)}(b)| = |B_{\pi(k)}|$, $(\dagger)$ implies $|A_k| \leqslant |B_{\pi(k)}|$. Since $\sum |A_k| = n = \sum |B_{\pi(k)}|$, we must have $|A_k| = |B_{\pi(k)}|$ for all k. Therefore, b is the π-image of a. □

6.6 Analysis of Small Ring Links (Base Case for Lemma 6.4)

We prove Lemma 6.4 by induction on n. This section establishes the base case $n = 4$, formalized as Claim 6.7. This relies on the intrinsic symmetry groups of $R(0101)$ and $R(1010)$.

6.6.1 Intrinsic Symmetry Groups

We use $\mathbb{Z}_2 = \{-1, 1\}$. For an oriented knot K, $(-1) \cdot K$ is K with reversed orientation.

Intrinsic symmetry relates to isotopies that map a link to itself or its mirror image, possibly permuting components and reversing orientations. Let L have components $L_1, \ldots, L_n$, and mirror image L^*. Let $(\epsilon_1, \ldots, \epsilon_n) \in \mathbb{Z}_2^n$ and $\pi \in S_n$.

(1) *L admits* $(1, \epsilon_1, \ldots, \epsilon_n, \pi)$ if an isotopy maps L to itself, taking L_i to $\epsilon_i \cdot L_{\pi(i)}$.

(2) *L admits* $(-1, \epsilon_1, \ldots, \epsilon_n, \pi)$ if an isotopy maps L to L^*, taking L_i to $\epsilon_i \cdot L^*_{\pi(i)}$.

The set of these tuples forms the *intrinsic symmetry group* of L [35]. For positive links, case (2) is irrelevant as the mirror image is not positive.

Figure 6.6 illustrates how $\mathcal{H}$ maps $R(0101)$ to $R(1010)$. If orientations are ignored, $\mathcal{H}$ maps the link to itself. Reconsidering orientations, $\mathcal{H}$ maps $R(0101)_i$ to $(-1)\cdot R(0101)_i$. Thus, $R(0101)$ admits the symmetry $(1,-1,-1,-1,-1,\iota)$.

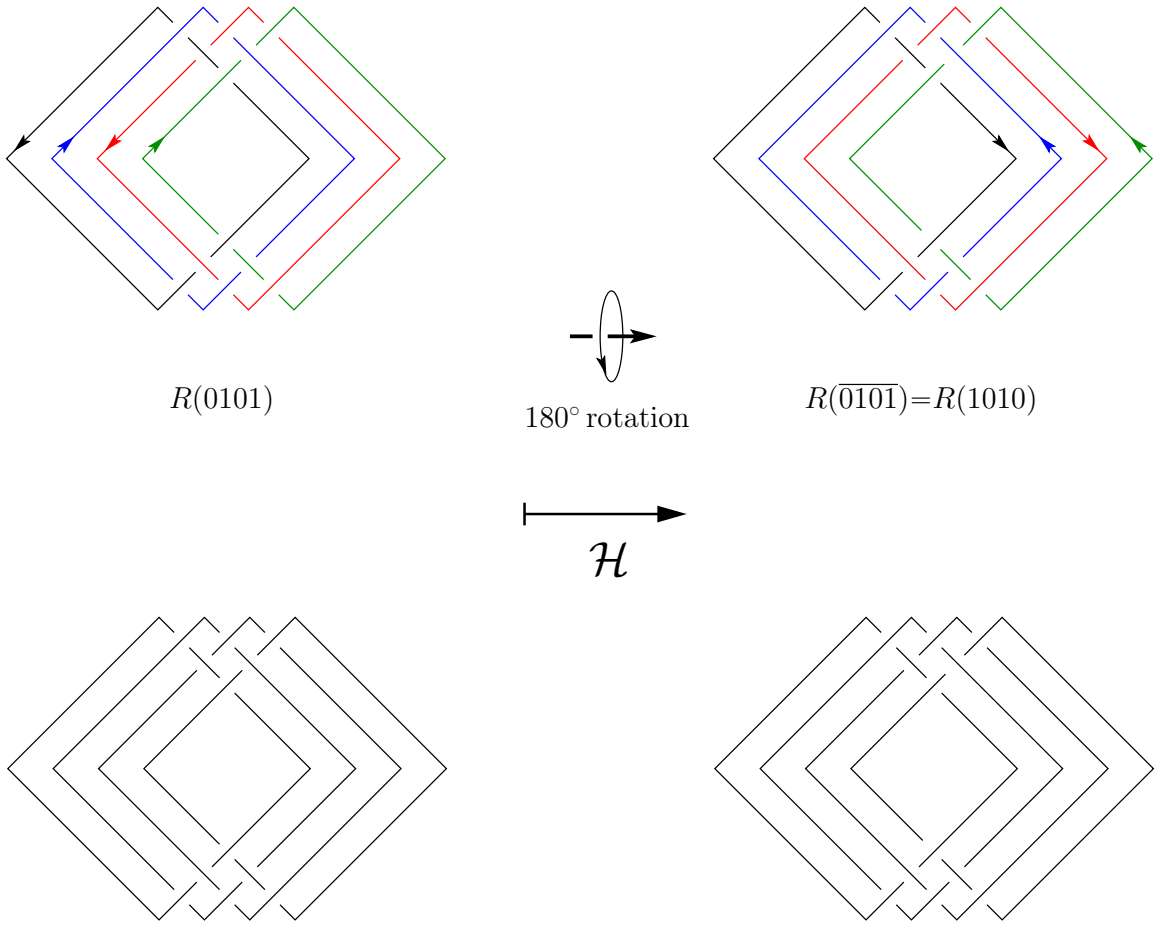

Figure 6.6: The isotopy $\mathcal{H}$ takes $R(0101)$ to $R(1010)$. Ignoring orientations (bottom), $\mathcal{H}$ takes $R(0101)$ to itself. This means $\mathcal{H}$ takes $R(0101)_i$ to $(-1)\cdot R(0101)_i$, witnessing the intrinsic symmetry $(1,-1,-1,-1,-1,(1\,2\,3\,4))$.

6.6.2 Symmetry Groups of Small Oscillating Ring Links

Calculating intrinsic symmetry groups is generally hard [4,5,24]. For small hyperbolic links [19], it can be computed using `SnapPy` [8] by analyzing the mapping class group of the complement.

$R(0101)$ and $R(1010)$ are hyperbolic. We used `SnapPy` following [5, Section 3] to compute their groups.

Fact 6.6. ([27]) The intrinsic symmetry group of $R(0101)$ (and $R(1010)$) is isomorphic to $\mathbb{Z}_2\times\mathbb{Z}_2$. Its elements are $(1,1,1,1,1,\iota)$, $(1,-1,-1,-1,-1,\iota)$, $(1,1,1,1,1,\nu)$, and $(1,-1,-1,-1,-1,\nu)$.

These symmetries correspond to the identity, $\mathcal{H}$, $\mathcal{V}$, and $\mathcal{V}\circ\mathcal{H}$, respectively.

6.6.3 The Base Case of Lemma 6.4

The following claim establishes the base case $n=4$ for Lemma 6.4.

Claim 6.7. *([27]) Let a be an oscillating word of length 4. Let $R(a) \sim R(b)$ via isotopy $\mathcal{I}$. Then,*

(1) b is oscillating; and

(2) the $(R(a), R(b))$-permutation under $\mathcal{I}$ is either ι or ν.

Proof. (1) states that if $a \in \{0101, 1010\}$ and $R(a) \sim R(b)$, then $b \in \{0101, 1010\}$. We verified this using `SnapPy` and `SageMath` by computing Jones polynomials (see Appendix). $V_{R(0101)}$ and $V_{R(1010)}$ are identical and distinct from all other 4-component ring links.

(2) Suppose $b = a$. Let π be the permutation under $\mathcal{I}$. Since $\mathcal{I}$ preserves orientations, $(1, 1, 1, 1, 1, \pi)$ is an intrinsic symmetry of $R(a)$. By Fact 6.6, $\pi \in \{\iota, \nu\}$.

Suppose $b = \overline{a}$. $\mathcal{I}$ maps $R(a)$ to $R(\overline{a})$, reversing all orientations. Thus $(1, -1, -1, -1, -1, \pi)$ is an intrinsic symmetry of $R(a)$. By Fact 6.6, $\pi \in \{\iota, \nu\}$. □

6.7 Proof of Lemma 6.4 (Inductive Step)

The proof relies on the equivalence between sublinks and smaller ring links.

6.7.1 Sublinks of Ring Links are Equivalent to Ring Links

Let $a_{i_1} \cdots a_{i_k}$ be a subword of a. The structure of $\mathscr{R}_n$ implies that the sublink $R(a)_{i_1,\ldots,i_k}$ is equivalent to the ring link $R(a_{i_1} \cdots a_{i_k})$ via a strong isotopy (Figure 6.7). This isotopy preserves the order of the components.

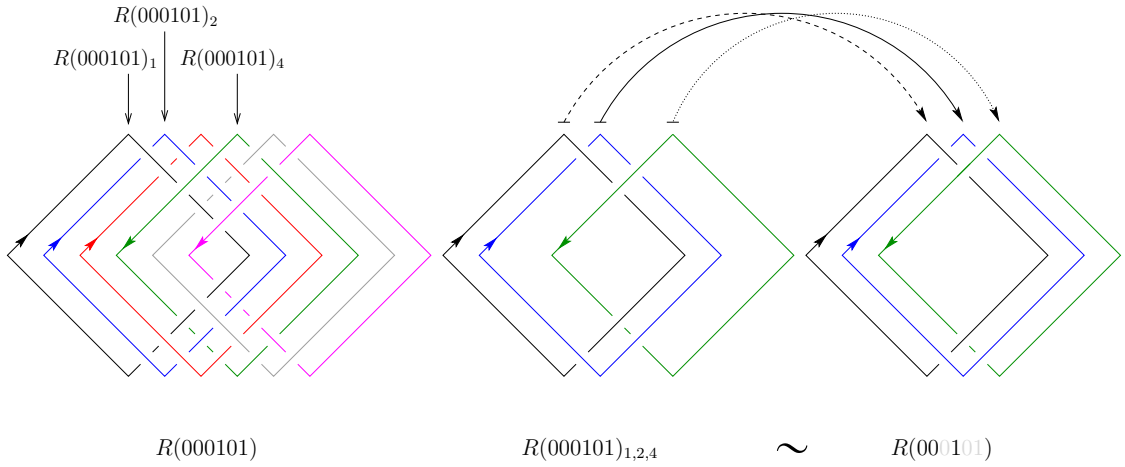

Figure 6.7: Illustration of Observation 6.8. The sublink $R(000101)_{1,2,4}$ (center) is strongly isotopic to the ring link $R(001)$.

This process is reversible.

Observation 6.8. *([27]) If $a_{i_1} \cdots a_{i_k}$ is a subword of a, then there exist $R(a)_{i_1,\ldots,i_k} \overset{\iota}{\longmapsto} R(a_{i_1} \cdots a_{i_k})$ and $R(a_{i_1} \cdots a_{i_k}) \overset{\iota}{\longmapsto} R(a)_{i_1,\ldots,i_k}$ isotopies.*

This leads to a crucial relationship used repeatedly.

Observation 6.9. *([27]) Let a, b be words. An $R(a)_{i_1,\ldots,i_k} \overset{\pi}{\longmapsto} R(b)_{j_1,\ldots,j_k}$ isotopy exists if and only if an $R(a_{i_1} \cdots a_{i_k}) \overset{\pi}{\longmapsto} R(b_{j_1} \cdots b_{j_k})$ isotopy exists.*

Proof. This follows from Observation 6.8 and the composition property (Observation 2.14). If $\mathcal{I}$ is the latter isotopy, we compose it with the strong isotopies relating the ring links to the sublinks ($\mathcal{J}$ and $\mathcal{K}$ from Observation 6.8) to obtain the former isotopy $\mathcal{K} \circ \mathcal{I} \circ \mathcal{J}$. The permutation remains $\iota \circ \pi \circ \iota = \pi$. □

6.7.2 Inductive Proof

It is easier to prove the following equivalent statement, formulated in terms of ring links (equivalence follows from Observation 6.9).

Lemma 6.10 ([27] Equivalent to Lemma 6.4)**.** *Let a be an oscillating word of length $n \geqslant 4$. Let $R(a) \sim R(b)$ via isotopy $\mathcal{I}$. Then,*

(1) the $(R(a), R(b))$-permutation under $\mathcal{I}$ is ι or ν; and

(2) b is oscillating.

Proof. We use induction on n. Claim 6.7 establishes the base case $n = 4$. Assume the lemma holds for length $m \geqslant 4$, and consider length $m + 1$.

Let $a = a_1 \cdots a_{m+1}$ be oscillating, $R(a) \sim R(b)$ via $\mathcal{I}$, and π the induced permutation. We must show (I) $\pi \in \{\iota, \nu\}$ and (II) b is oscillating.

Consider the sublinks $R(a)_{1,\ldots,m}$ and $R(a)_{2,\ldots,m+1}$. By Observation 6.9 and the induction hypothesis, the permutation induced by $\mathcal{I}$ on $R(a)_{1,\ldots,m}$ is either (i) ι or (ii) ν. Similarly, on $R(a)_{2,\ldots,m+1}$ it is either (iii) ι or (iv) ν.

(i) implies $\pi(1) < \cdots < \pi(m)$. (ii) implies $\pi(1) > \cdots > \pi(m)$. (iii) implies $\pi(2) < \cdots < \pi(m+1)$. (iv) implies $\pi(2) > \cdots > \pi(m+1)$.

The combinations (i) and (iv) are contradictory, as are (ii) and (iii). Thus, either [(i) and (iii)] or [(ii) and (iv)] must hold.

If (i) and (iii) hold, then $\pi(1) < \pi(2) < \cdots < \pi(m+1)$, so $\pi = \iota$. If (ii) and (iv) hold, then $\pi(1) > \pi(2) > \cdots > \pi(m+1)$, so $\pi = \nu$. Thus (I) holds.

To prove (II), assume $\pi = \nu$ (the case $\pi = \iota$ is analogous). Then $\mathcal{I}$ maps $R(a)_{1,\ldots,m}$ to $R(b)_{2,\ldots,m+1}$ (†), and $R(a)_{2,\ldots,m+1}$ to $R(b)_{1,\ldots,m}$ (‡).

By Observation 6.9 and the induction hypothesis (Part 2), (†) implies $R(b)_{2,\ldots,m+1}$ is oscillating ($*$). Similarly, (‡) implies $R(b)_{1,\ldots,m}$ is oscillating ($**$). Combining ($*$) and ($**$) ensures b is oscillating. □

Chapter 7

Flower Links

We refer to a link in $\overrightarrow{\mathcal{L}}^+(\mathscr{F}_n)$ as a *flower link of size n*. We employ the same proof strategy used for ring and boot links.

For convenience, we restrict our analysis primarily to flower links of even size. This avoids complexities in several arguments without affecting the validity of the asymptotic result in Theorem 1.4 (as shown by Proposition 7.5 and Corollary 7.6).

Remark. *([27]) When analyzing flower links, it is implicitly assumed they have an* even *number of components.*

7.1 Correspondence Between Flower Links and Binary Words

A flower link of size n corresponds to a binary word of length n. Unlike the linear ordering of ring and boot arrangements, flower arrangements are cyclic and require a labeling convention. For an even n, $\mathscr{F}_n$ has two topmost pseudocircles. We order them $1, \ldots, n$ starting with the *topmost right* component and proceeding clockwise (Figure 7.1).

The orientation is encoded by a word a, defining the oriented arrangement $\mathscr{F}_n(a)$ and the induced positive link $F(a)$ (where F stands for "flower"). Thus, *there is a bijection between binary words of length n and the collection* $\overrightarrow{\mathcal{L}}^+(\mathscr{F}_n)$.

7.2 Isotopies Acting Naturally on Flower Links

We identify natural isotopies that establish equivalences between flower links (Observation 7.1), and then prove these are the only equivalences (Proposition 7.5).

7.2.1 Rotational Isotopy and Cyclic Shifts

We define $\mathcal{R}_{2\pi/n}$ as the isotopy corresponding to a clockwise rotation by $2\pi/n$ ($360^\circ/n$) around the center (Figure 7.2).

Applying $\mathcal{R}_{2\pi/n}$ to $F(a_1 \cdots a_n)$ yields $F(a_n a_1 \cdots a_{n-1})$. We define the corresponding word mapping $\mathbf{r}$ (rotation) as $\mathbf{r}(a_1 \cdots a_n) = a_n a_1 \cdots a_{n-1}$. Thus, $\mathcal{R}_{2\pi/n} \,\big|\, F(a) \to F(\mathbf{r}(a))$.

The induced permutation is the cyclic shift $(2\,3 \cdots n\ 1)$, denoted σ. We have:

$$\mathcal{R}_{2\pi/n} \,\big|\, F(a) \xrightarrow{\sigma} F(\mathbf{r}(a)).$$

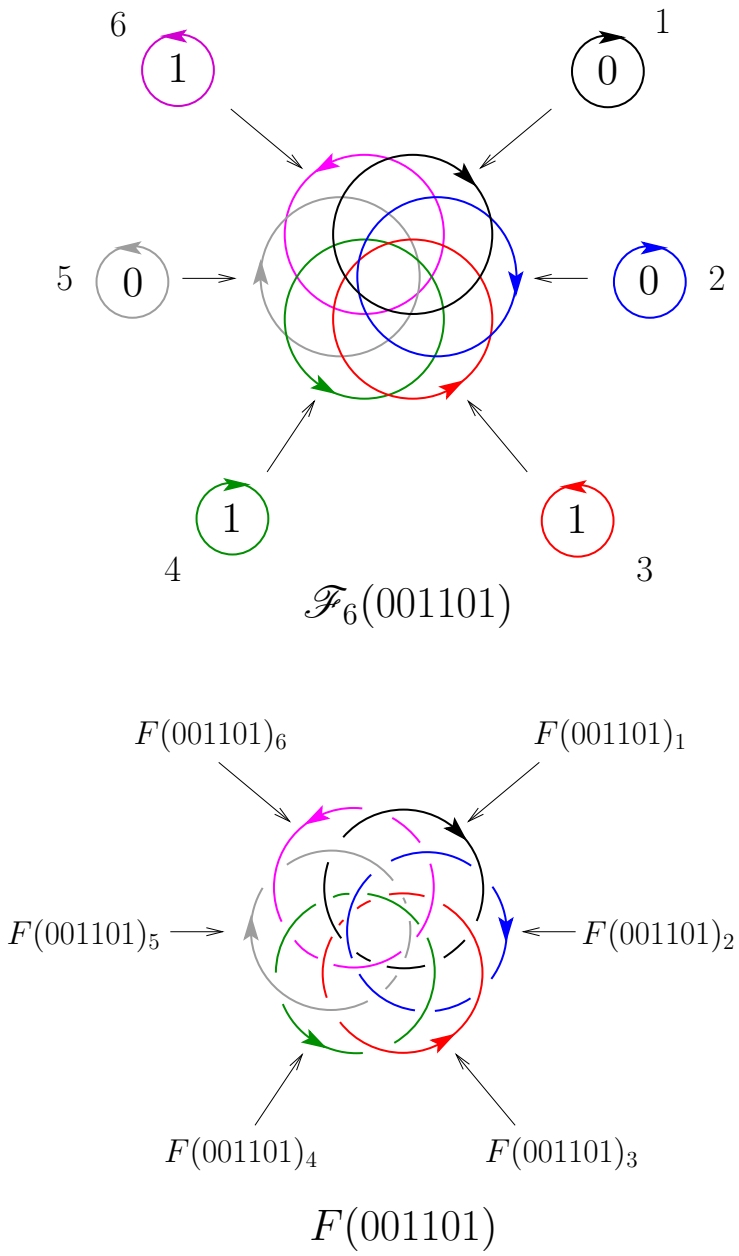

Figure 7.1: The oriented arrangement $\mathscr{F}_6(001101)$ and its induced link, the flower link $F(001101)$.

To describe the action of iterated shifts σ^s, we introduce modular notation.

Notation. ([27]) $p \oplus_n q$ *is* $(p+q) \pmod n$, *adjusted to be in* $\{1, \ldots, n\}$. *(Specifically,* n *if* $p+q \equiv 0 \pmod n$*).*

Then $\sigma^s(i) = i \oplus_n s$. The isotopy $\mathcal{R}_{2\pi/n}$ maps $F(a)_i$ to $F(\mathbf{r}a)_{i \oplus_n 1}$.

The s-fold iteration $\mathcal{R}^s_{2\pi/n}$ corresponds to the word mapping $\mathbf{r}^s$ and induces the permutation σ^s. Note that $\mathcal{R}^n_{2\pi/n}$ is the identity isotopy.

7.2.2 The Vertical Isotopy $\mathcal{V}$ and the Word Mapping v

The isotopy $\mathcal{V}$ (vertical axis rotation, used for ring links) also acts on flower links. Applying $\mathcal{V}$ to $F(a)$ yields $F((\overline{a})^{-1}) = F(\overline{a_n \cdots a_1})$ (Figure 7.3).

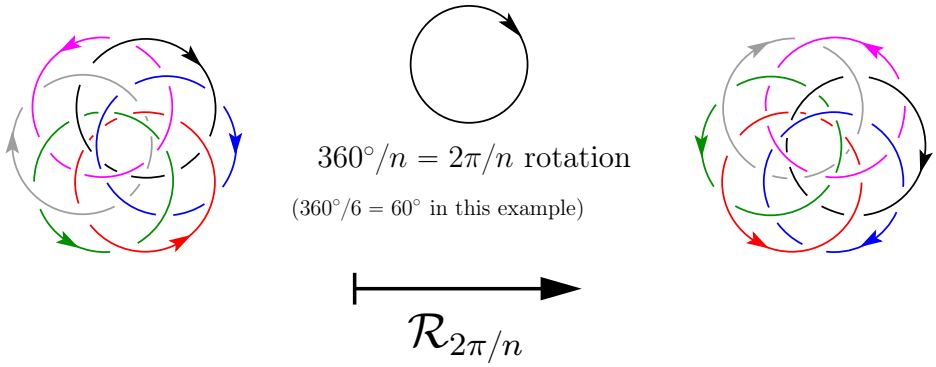

Figure 7.2: The isotopy $\mathcal{R}_{2\pi/n}$ takes $F(a_1 \cdots a_n)$ to $F(a_n a_1 \cdots a_{n-1})$. Here $\mathcal{R}_{2\pi/6}$ takes $F(001101)$ to $F(100110)$. The induced permutation is the cyclic shift $\sigma = (2\,3 \cdots n\,1)$.

We define the word mapping $\mathbf{v}$ as $\mathbf{v}(a) = (\overline{a})^{-1}$. Thus $\mathcal{V} \,|\, F(a) \to F(\mathbf{v}(a))$. The induced permutation is the reverse permutation ν. $\mathcal{V} \,|\, F(a) \xrightarrow{\nu} F(\mathbf{v}(a))$.

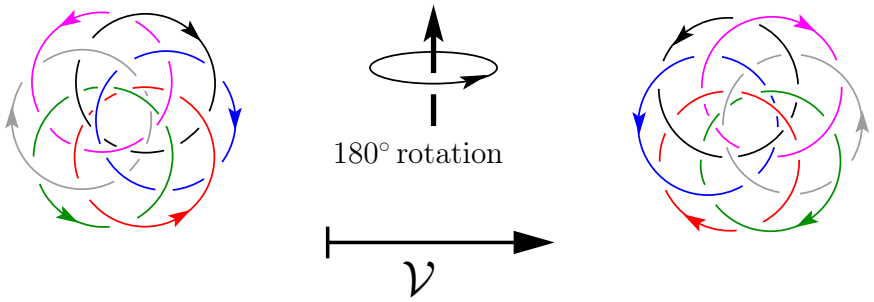

Figure 7.3: Applying $\mathcal{V}$ to $F(001101)$ yields $F(\mathbf{v}(001101)) = F(010011)$. The induced permutation is ν.

7.2.3 Sufficient Conditions for Equivalence

If $F(b)$ is obtained from $F(a)$ by any sequence of $\mathcal{R}_{2\pi/n}$ and $\mathcal{V}$ isotopies, then $F(a) \sim F(b)$. This corresponds to applying sequences of $\mathbf{r}$ and $\mathbf{v}$ operations to the word a.

Definition. ([27]) *We say b is* related *to a, written $a \equiv b$, if b can be obtained from a by a sequence of $\mathbf{r}$ and $\mathbf{v}$ operations.*

Observation 7.1. *([27]) If $a \equiv b$, then $F(a) \sim F(b)$.*

7.2.4 Properties of the Relation $\equiv$

The operations $\mathbf{r}$ and $\mathbf{v}$ generate a group $\langle \mathbf{r}, \mathbf{v} \rangle$ isomorphic to the dihedral group D_n, reflecting the symmetries of a regular n-gon generated by rotation and reflection.

Remark 7.2. ([27]) $\equiv$ *is an equivalence relation.*

The group $\langle \mathbf{r}, \mathbf{v} \rangle$ has $2n$ elements, expressible as $\mathbf{r}^s$ or $\mathbf{r}^s \circ \mathbf{v}$ for $s \in \{0, \ldots, n-1\}$.

Remark 7.3. ([27]) $a \equiv b$ if and only if $b = \mathbf{r}^s(a)$ or $b = \mathbf{r}^s \circ \mathbf{v}(a)$ for some s. The equivalence class of a has size at most $2n$.

If $a = D_1 D_2$, the word $b = D_2 D_1$ is a *shift* of a. A shift is achieved by applying $\mathbf{r}$ repeatedly.

Remark 7.4. ([27]) If b is a shift of a, then $b \equiv a$.

7.3 Reduction of Theorem 1.4

The main step in proving Theorem 1.4 is establishing the converse of Observation 7.1 when the rank is high enough.

Proposition 7.5. *([27]) Let a be a word of even rank $r \geqslant 6$. If $F(a) \sim F(b)$, then $b \equiv a$.*

We defer the proof and extend this result to odd ranks.

Corollary 7.6. *([27]) Let a be a word of rank $r \geqslant 6$. If $F(a) \sim F(b)$, then $b \equiv a$.*

Proof. If r is even, Proposition 7.5 applies. Assume r is odd ($r \geqslant 7$). Let $a = A_1 \cdots A_r$ be the canonical decomposition. Since r is odd, $A_r A_1$ is monotone. Let $a' = A_2 \cdots A_{r-1}(A_r A_1)$. a' is a shift of a, so $a' \equiv a$, and $F(a') \sim F(a)$. Since $F(a) \sim F(b)$, we have $F(a') \sim F(b)$. The rank of a' is $r - 1$, which is even and $\geqslant 6$. By Proposition 7.5, $a' \equiv b$. By transitivity, $a \equiv b$. □

Proof of Theorem 1.4 (assuming Proposition 7.5). Let a be a word of length n. As $n \to \infty$, the probability that $\mathrm{rank}(a) < 6$ approaches 0. The probability that the equivalence class of a under $\equiv$ has size less than $2n$ also approaches 0. By Observation 7.1 and Corollary 7.6, the probability that exactly $2n$ words b satisfy $F(a) \sim F(b)$ approaches 1. Thus, the expected size of an equivalence class in $\overrightarrow{\mathcal{L}}^+(\mathscr{F}_n)$ is $2n$. Since $|\overrightarrow{\mathcal{L}}^+(\mathscr{F}_n)| = 2^n$, Theorem 1.4 follows. □

7.4 Proof of Proposition 7.5

We analyze sublinks of flower links and reduce Proposition 7.5 to two lemmas.

7.4.1 Sublinks of Flower Links

A subword $a_{i_1} \cdots a_{i_k}$ corresponds to the sublink $F(a)_{i_1,\ldots,i_k}$. $F(a)$ (or a sublink) is *oscillating* if the corresponding word (or subword) is oscillating.

7.4.2 Reduction to Lemmas

We reduce Proposition 7.5 to the following lemmas, analogous to the previous cases.

Lemma 7.7. *([27]) Let a, b have the same even rank $r \geqslant 6$. If $F(a) \sim F(b)$ via $\mathcal{I}$. Let $F(a)_{i_1,\ldots,i_r}$ be oscillating, and $F(b)_{j_1,\ldots,j_r}$ its image. Then b is the π-image of a, where π is the induced permutation.*

Lemma 7.8. *([27]) Let a have even rank $r \geqslant 6$, and $F(a)_{i_1,\ldots,i_r}$ be oscillating. Let $F(a) \sim F(b)$ via $\mathcal{I}$, and $F(b)_{j_1,\ldots,j_r}$ be the image of $F(a)_{i_1,\ldots,i_r}$. Then,*

(1) the induced permutation π is σ^s or $\sigma^s \circ \nu$ for some $s \in \{0, \ldots, r-1\}$; and

(2) if s is even, $b_{j_1} \cdots b_{j_r} = a_{i_1} \cdots a_{i_r}$; if s is odd, $b_{j_1} \cdots b_{j_r} = \overline{a_{i_1} \cdots a_{i_r}}$.

In particular, $F(b)_{j_1,\ldots,j_r}$ is oscillating.

We first note a consequence regarding the rank.

Corollary 7.9. *([27]) Let a have even rank $r \geqslant 6$. If $F(a) \sim F(b)$, then* $\mathrm{rank}(b)$ *is r or $r+1$. If* $\mathrm{rank}(b)$ *is even,* $\mathrm{rank}(b) = r$.

Proof. Let $s := \mathrm{rank}(b)$. Lemma 7.8 implies $s \geqslant r$. If s is even, applying the lemma symmetrically implies $r \geqslant s$, so $r = s$. If s is odd, assume $s > r+1$. There is a shift b' of b with rank $s-1$ (even). $F(b') \sim F(a)$. Applying Lemma 7.8 to $F(b') \mapsto F(a)$ implies $F(a)$ has an oscillating sublink of size $s-1$. This contradicts $\mathrm{rank}(a) = r$, since $s - 1 > r$. □

Proof of Lemma 7.7 (assuming Lemma 7.8). The proof is virtually identical to that of Lemma 6.3, substituting F for R, Corollary 7.9 for Corollary 6.5, and Lemma 7.8(2) for Lemma 6.4(2). □

Proof of Proposition 7.5 (assuming Lemma 7.8). Let a have even rank $r \geqslant 6$, and $F(a) \sim F(b)$. Lemma 7.7 requires both words to have the same even rank.

By Corollary 7.9, $\mathrm{rank}(b) \in \{r, r+1\}$. If $\mathrm{rank}(b) = r$, let $c = b$. If $\mathrm{rank}(b) = r+1$, let c be the shift of b such that $\mathrm{rank}(c) = r$ (as in Corollary 7.6). In both cases, c has even rank r, and $c \equiv b$. We aim to show $c \equiv a$, which implies $b \equiv a$.

Since $F(c) \sim F(a)$, let π be the permutation induced on an oscillating sublink $F(a)_{i_1,\ldots,i_r}$. Let $a = A_1 \cdots A_r$ and $c = C_1 \cdots C_r$ be canonical decompositions.

By Lemma 7.7, c is the π-image of a. By Lemma 7.8 (1), π is σ^s or $\sigma^s \circ \nu$.

Case 1: $\pi = \sigma^s$. Then $|C_{k \oplus_r s}| = |A_k|$. If s is even, Lemma 7.8 (2) implies the underlying oscillating words are equal. Combined with the matching lengths, a is a shift of c. Thus $c \equiv a$. If s is odd, Lemma 7.8 (2) implies the underlying oscillating words are negations of each other. However, since r is even, an odd shift of an oscillating word is its negation. Analyzing the structure shows a is still a shift of c. Thus $c \equiv a$.

Case 2: $\pi = \sigma^s \circ \nu$. Then $|C_{\pi(k)}| = |A_k|$. Analyzing the structure based on the parity of s and applying Lemma 7.8 (2), we find that a corresponds to a shift of $\mathbf{v}(c) = (\overline{c})^{-1}$. Since $a \equiv \mathbf{v}(c)$ and $\mathbf{v}(c) \equiv c$, we have $c \equiv a$. □

7.5 Analysis of Small Flower Links (Base Case for Lemma 7.8)

We prove Lemma 7.8 by induction. This section establishes the base case $n = 6$ (Claim 7.11).

7.5.1 Symmetry Groups of $F(010101)$ and $F(101010)$

We need the intrinsic symmetry groups of $F(010101)$ and $F(101010)$. These are hyperbolic, computed via `SnapPy`.

The results involve two key symmetries. Consider $F(010101)$. The isotopy $\mathcal{R}_{2\pi/6}$ maps $F(010101)$ to $F(101010)$ (Figure 7.4). Ignoring orientations, it maps the link to itself. With orientations, it maps $F(010101)_i$ to $-1 \cdot F(010101)_{i \oplus_6 1}$. This witnesses the symmetry $(1, -1, -1, -1, -1, -1, -1, \sigma)$.

The isotopy $\mathcal{V}$ maps $F(010101)$ to $F(\mathbf{v}(010101)) = F(010101)$ (Figure 7.5). It preserves orientations and induces the reverse permutation ν. This witnesses the symmetry $(1, 1, 1, 1, 1, 1, 1, \nu)$.

Fact 7.10. ([27]) The intrinsic symmetry group of $F(010101)$ (and $F(101010)$) is isomorphic to the dihedral group D_6, generated by $(1, -1, -1, -1, -1, -1, -1, \sigma)$ and $(1, 1, 1, 1, 1, 1, 1, \nu)$.

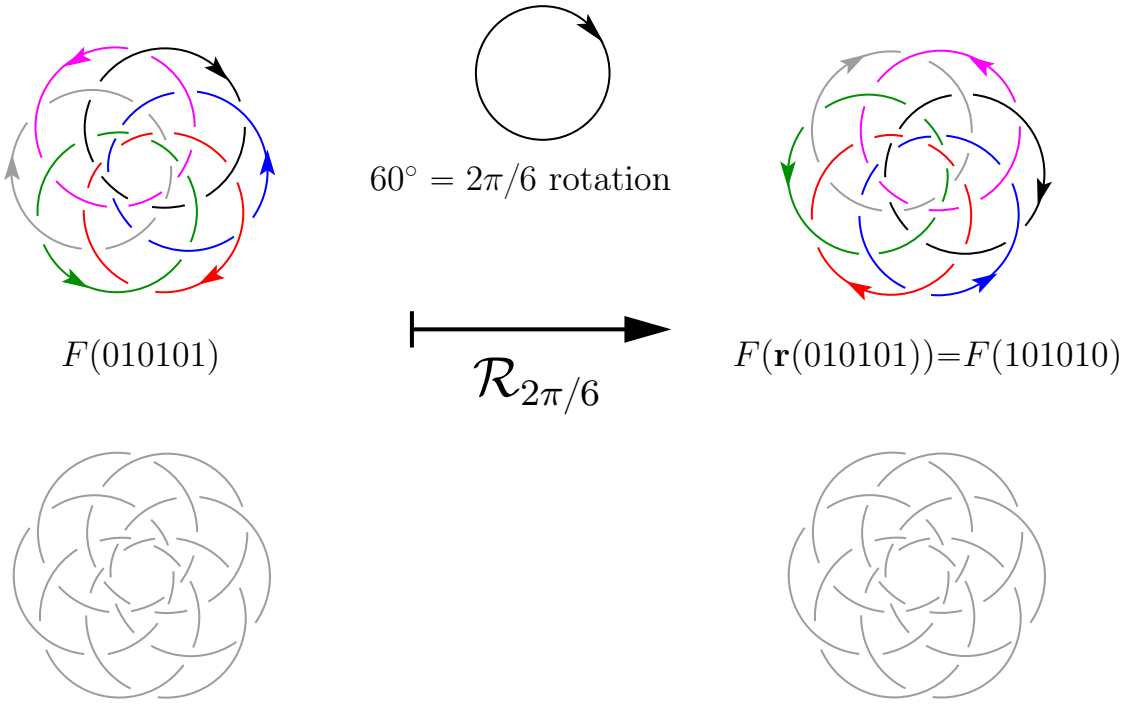

Figure 7.4: $\mathcal{R}_{2\pi/6}$ takes $F(010101)$ to $F(101010)$. This witnesses a intrinsic symmetry.

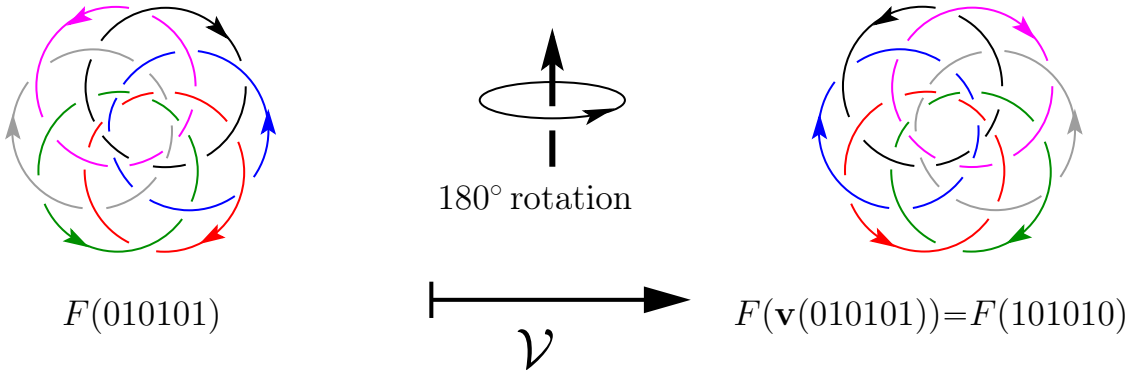

Figure 7.5: $\mathcal{V}$ takes $F(010101)$ to itself while preserving orientations. This witnesses a intrinsic symmetry.

7.5.2 The Base Case

Claim 7.11. *([27]) Let a be an oscillating word of length 6. Let $F(a) \sim F(b)$ via isotopy $\mathcal{I}$. Then,*

(1) the induced permutation π is σ^s or $\sigma^s \circ \nu$ for some $s \in \{0, \ldots, 5\}$; and

(2) if s is even, $b = a$; if s is odd, $b = \overline{a}$.

If an isotopy $\mathcal{I}$ induces an intrinsic symmetry $(1, \epsilon_1, \ldots, \epsilon_n, \pi)$, we call $(\epsilon_1, \ldots, \epsilon_n, \pi)$ the *stamp of $\mathcal{I}$ over L*.

Proof. We first verify b is oscillating. Using `SnapPy` and `SageMath` (see Appendix), the Jones polynomial confirms that if $F(a) \sim F(b)$, then $b \in \{a, \overline{a}\}$.

Let π be the permutation under $\mathcal{I}$. Since $F(a)$ and $F(b)$ are equivalent unoriented, $\mathcal{I}$ has a stamp $\Theta = (\epsilon_1, \ldots, \epsilon_6, \pi)$. $(1, \Theta)$ is an intrinsic symmetry of $F(a)$. By Fact 7.10, Θ must be of

the form $((-1)^s, \ldots, (-1)^s, \sigma^s)$ or $((-1)^s, \ldots, (-1)^s, \sigma^s \circ \nu)$. This proves (1).

If s is even, $\epsilon_i = 1$ for all i. $\mathcal{I}$ preserves orientations, so $b = a$. If s is odd, $\epsilon_i = -1$ for all i. $\mathcal{I}$ reverses orientations, so $b = \overline{a}$. This proves (2). □

7.6 Proof of Lemma 7.8 (Inductive Step)

We rely on the properties of sublinks of flower links.

7.6.1 Sublinks of Flower Links are Equivalent to Flower Links

The sublink $F(a)_{i_1,\ldots,i_k}$ is strongly isotopic to the flower link $F(a_{i_1} \cdots a_{i_k})$ (Figure 7.6).

Observation 7.12. *([27]) If $a_{i_1} \cdots a_{i_k}$ is a subword of a, then there exist $F(a)_{i_1,\ldots,i_k} \overset{\iota}{\longmapsto} F(a_{i_1} \cdots a_{i_k})$ and $F(a_{i_1} \cdots a_{i_k}) \overset{\iota}{\longmapsto} F(a)_{i_1,\ldots,i_k}$ isotopies.*

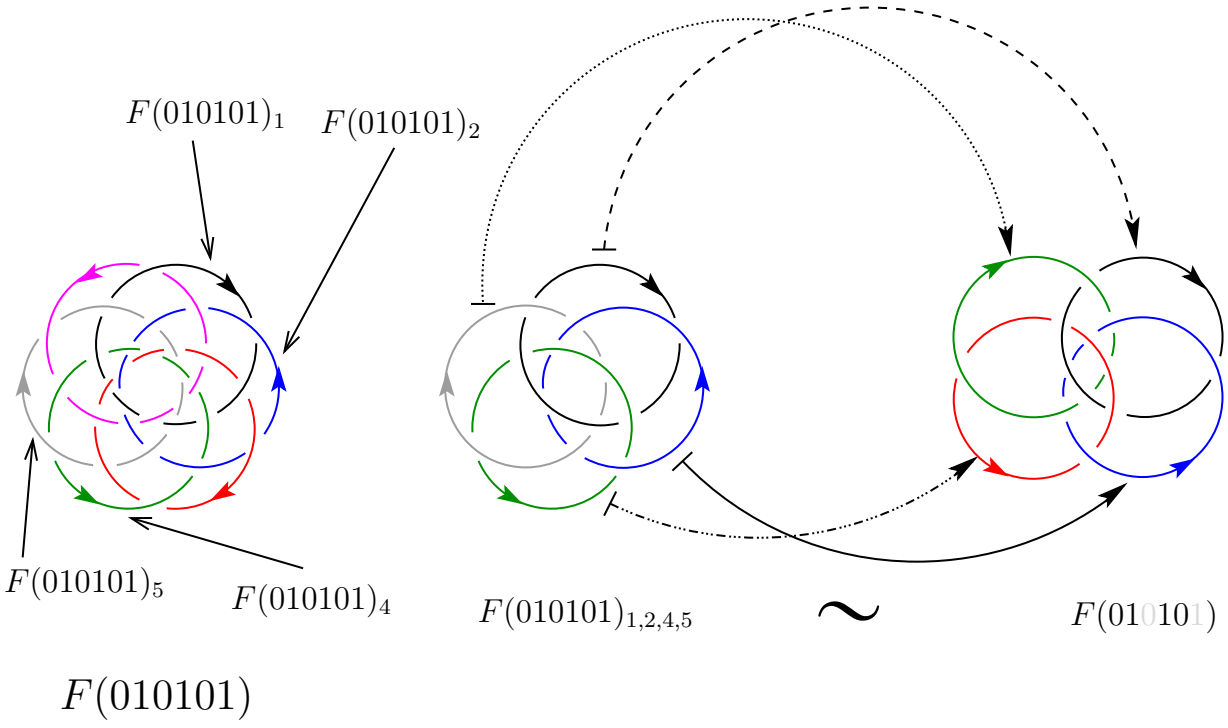

Figure 7.6: Illustration of Observation 7.12.

Observation 7.13. *An $F(a)_{i_1,\ldots,i_k} \overset{\pi}{\longmapsto} F(b)_{j_1,\ldots,j_k}$ isotopy exists if and only if: an $F(a_{i_1} \cdots a_{i_k}) \overset{\pi}{\longmapsto} F(b_{j_1} \cdots b_{j_k})$ isotopy exists.*

7.6.2 Inductive Proof

We prove the equivalent Lemma 7.14.

Lemma 7.14 (([27]) Equivalent to Lemma 7.8)**.** *Let a be an oscillating word of even length $n \geqslant 6$. If $F(a) \sim F(b)$ via isotopy $\mathcal{I}$, then (1) the induced permutation π is σ^s or $\sigma^s \circ \nu$; and (2) $b = a$ (s even) or $b = \overline{a}$ (s odd).*

We use the concepts of *n-consistent* (a cyclic shift is increasing) and *n-anticonsistent* (a cyclic shift is decreasing) sequences.

Remark 7.15. ([27]) A permutation $(j_1 \cdots j_n)$ is σ^s (resp. $\sigma^s \circ \nu$) if the sequence $j_1, \ldots, j_n$ is n-consistent (resp. n-anticonsistent).

Proof of Lemma 7.8. We use induction on the even length n. Claim 7.11 is the base case $n = 6$. Assume it holds for $m \geqslant 6$, and consider $m + 2$.

Let a be oscillating of length $m + 2$, $F(a) \sim F(b)$ via $\mathcal{I}$ with permutation π.

We note structural properties of a since m is even: (§) $a_1 \cdots a_m = (a_1 a_2)^{m/2}$. (§§) $a_3 \cdots a_{m+2} = (a_1 a_2)^{m/2}$.

Consider an oscillating sublink $F(a)_{i_1,\ldots,i_m}$. By the induction hypothesis, the permutation induced by $\mathcal{I}$ on this sublink is σ^s or $\sigma^s \circ \nu$. This means the image indices $\pi(i_1), \ldots, \pi(i_m)$ are $(m + 2)$-consistent or $(m + 2)$-anticonsistent, respectively.

Applying this to two distinct oscillating sublinks of size m, we find that the consistency or anticonsistency must align for both. If both are consistent, π is $(m + 2)$-consistent. If both are anticonsistent, π is $(m + 2)$-anticonsistent. By Remark 7.15, (I) holds: π is σ^s or $\sigma^s \circ \nu$.

To prove (II), we analyze the structure of b based on π. Suppose $\pi = \sigma^s$. We apply the induction hypothesis (Part 2) to the sublinks $F(a)_{1,\ldots,m}$ and $F(a)_{3,\ldots,m+2}$. By comparing the overlapping segments of b derived from these two applications (using § and §§), we determine that if s is even, $b = a$, and if s is odd, $b = \overline{a}$. The case $\pi = \sigma^s \nu$ follows similarly. □

Chapter 8

Boot Links

We refer to a link in $\overrightarrow{\mathcal{L}}^+(\mathscr{B}_n)$ as a *boot link of size n*. The proof of Theorem 1.3 utilizes the same strategy developed for Theorem 1.2, allowing for a more concise presentation.

8.1 Correspondence Between Boot Links and Binary Words

A boot link of size n is associated with a binary word of size n, encoded identically to ring links [27]. The pseudocircles in $\mathscr{B}_n$ are ordered $1, \ldots, n$ from left to right. The word a defines the orientations, yielding the oriented arrangement $\mathscr{B}_n(a)$ and the induced positive link $B(a)$ (Figure 8.1).

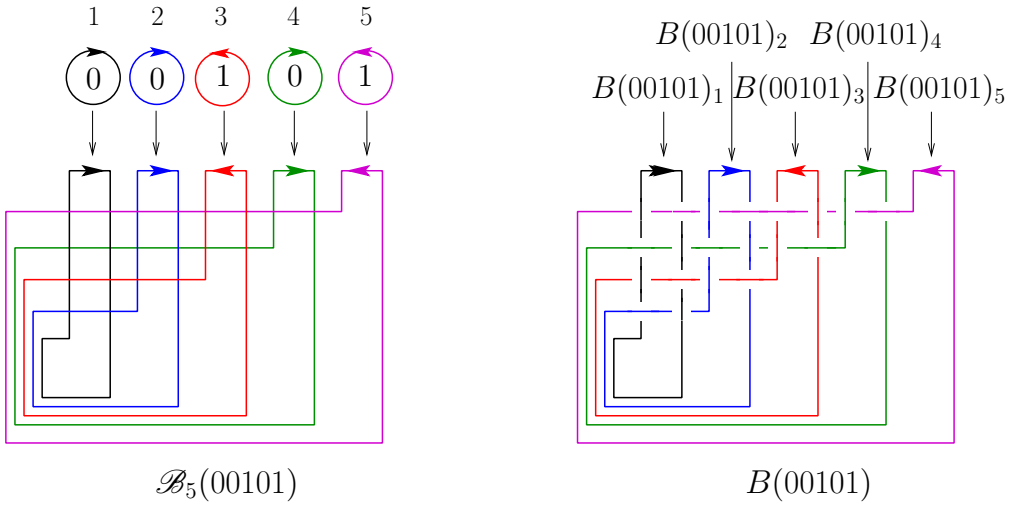

Figure 8.1: The oriented arrangement $\mathscr{B}_5(00101)$ and its induced positive link, the boot link $B(00101)$.

Thus, *there is a bijection between binary words of length n and the collection* $\overrightarrow{\mathcal{L}}^+(\mathscr{B}_n)$.

8.2 Reduction of Theorem 1.3

Unlike ring links, which exhibit natural isotopies corresponding to negation and reversal (Observation 6.1), boot links lack such symmetries. The analogue to Observation 6.1 is trivial:

$$(*)\ \textit{if } b = a, \textit{ then } B(a) = B(b).$$

The proof of Theorem 1.3 relies on establishing the converse of $(*)$ when the rank is sufficiently high.

Proposition 8.1. *([27]) Let a be a word of rank $r \geqslant 6$. If b is a word such that $B(a) \sim B(b)$, then $b = a$.*

Proof of Theorem 1.3 (assuming Proposition 8.1). Let a be a word of length n. The probability that $\text{rank}(a) < 6$ approaches 0 as $n \to \infty$. By Proposition 8.1, the probability that $B(a)$ is not equivalent to any other boot link approaches 1 as $n \to \infty$. This means the equivalence class of a random link in $\overrightarrow{\mathcal{L}}^+(\mathscr{B}_n)$ has size 1 with high probability. Since $|\overrightarrow{\mathcal{L}}^+(\mathscr{B}_n)| = 2^n$, Theorem 1.3 follows. □

8.3 Proof of Proposition 8.1

We analyze sublinks of boot links, following the methodology used for ring links.

8.3.1 Sublinks of Boot Links

A subword $a_{i_1} \cdots a_{i_k}$ corresponds to the sublink $B(a)_{i_1,\ldots,i_k}$. The link $B(a)$ (or sublink) is *oscillating* if the corresponding word (or subword) is oscillating.

Similar to ring links, the structure of $\mathscr{B}_n$ implies that the sublink $B(a)_{i_1,\ldots,i_k}$ is strongly isotopic to the boot link $B(a_{i_1} \cdots a_{i_k})$ (Figure 8.2).

Observation 8.2. *([27]) If $a_{i_1} \cdots a_{i_k}$ is a subword of a, then there exist $B(a)_{i_1,\ldots,i_k} \overset{\iota}{\longmapsto} B(a_{i_1} \cdots a_{i_k})$ and $B(a_{i_1} \cdots a_{i_k}) \overset{\iota}{\longmapsto} B(a)_{i_1,\ldots,i_k}$ isotopies.*

This yields the parallel to Observation 6.9.

Observation 8.3. *([27]) An $B(a)_{i_1,\ldots,i_k} \overset{\pi}{\longmapsto} B(b)_{j_1,\ldots,j_k}$ isotopy exists if and only if: an $B(a_{i_1} \cdots a_{i_k}) \overset{\pi}{\longmapsto} B(b_{j_1} \cdots b_{j_k})$ isotopy exists.*

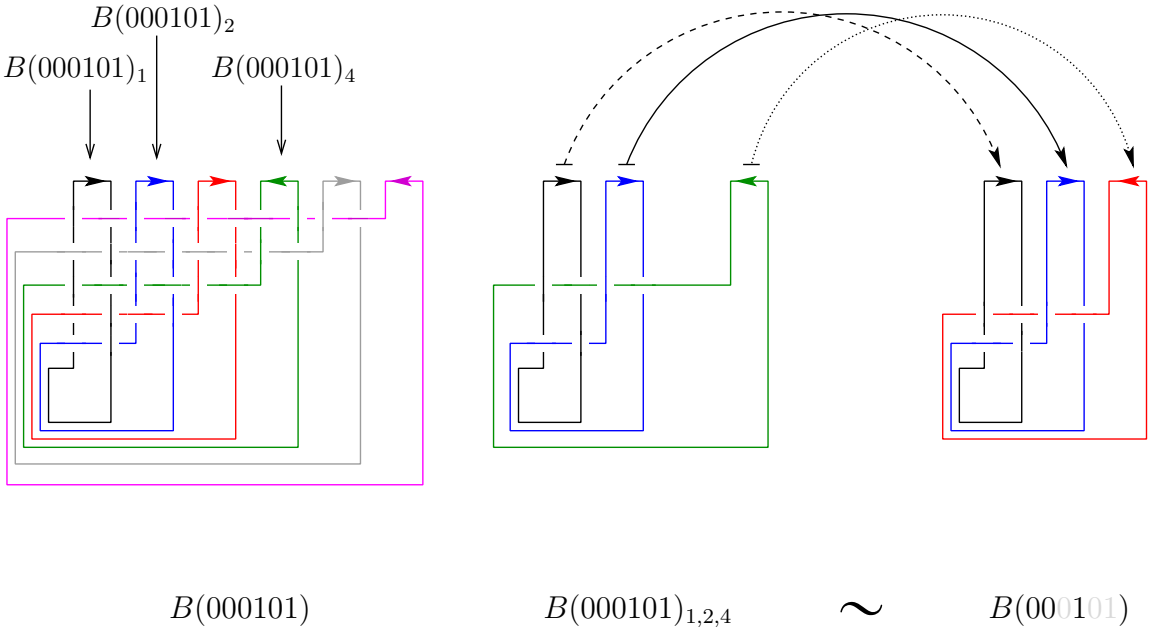

Figure 8.2: Illustration of Observation 8.2.

8.3.2 Reduction to Lemmas

We reduce Proposition 8.1 to the following lemmas, paralleling Lemmas 6.3 and 6.4.

Lemma 8.4. *([27]) Let a be a word with rank $r \geqslant 6$, $B(a) \sim B(b)$ via isotopy $\mathcal{I}$. Let $B(a)_{i_1,\ldots,i_r}$ be an oscillating sublink, and $B(b)_{j_1,\ldots,j_r}$ its image. Then b is the π-image of a, where π is the induced permutation.*

Lemma 8.5. *([27]) Let a have rank $r \geqslant 6$, and $B(a)_{i_1,\ldots,i_r}$ be an oscillating sublink. Let $B(a) \sim B(b)$ via $\mathcal{I}$, and $B(b)_{j_1,\ldots,j_r}$ be the image of $B(a)_{i_1,\ldots,i_r}$. Then,*

(1) the induced permutation is ι; and

(2) $b_{j_1} \cdots b_{j_r} = a_{i_1} \cdots a_{i_r}$.

We have the following consequence, analogous to Corollary 6.5.

Corollary 8.6. *([27]) Let a have rank $r \geqslant 6$. If $B(a) \sim B(b)$, then* $\mathrm{rank}(b) = r$.

Proof of Lemma 8.4 (assuming Lemma 8.5). The proof is virtually identical to that of Lemma 6.3, substituting B for R, Corollary 8.6 for Corollary 6.5, and Lemma 8.5(2) for Lemma 6.4(2). □

Proof of Proposition 8.1 (assuming Lemma 8.5). Let a have rank $r \geqslant 6$, $B(a) \sim B(b)$ via $\mathcal{I}$. Let $B(a)_{i_1,\ldots,i_r}$ be oscillating, $B(b)_{j_1,\ldots,j_r}$ its image, and π the induced permutation.

By Corollary 8.6, $\mathrm{rank}(b) = r$. Let $a = A_1 \cdots A_r$ and $b = B_1 \cdots B_r$ be the canonical decompositions.

Lemma 8.4 implies b is the π-image of a. Lemma 8.5(1) implies $\pi = \iota$. Thus $|B_k| = |A_k|$ and Lemma 8.5(2) implies $b_{j_1} \cdots b_{j_r} = a_{i_1} \cdots a_{i_r}$. Since both the sequence of bits and the lengths of the blocks match, $b = a$. □

8.4 Proof of Lemma 8.5

The proof is by induction on n. The base case $n = 6$ requires the intrinsic symmetry groups of $B(010101)$ and $B(101010)$. These links are hyperbolic, allowing computation via `SnapPy`.

Fact 8.7. ([27]) The intrinsic symmetry groups of $B(010101)$ and $B(101010)$ are trivial. Any self-isotopy induces the identity permutation ι.

We establish the base case (Claim 8.8).

Claim 8.8. *([27]) Let a be an oscillating word of length* 6. *If $B(a) \sim B(b)$ via isotopy $\mathcal{I}$, then,*

(1) $b = a$; and

(2) the induced permutation is ι.

Proof. (1) We prove the case $a = 010101$. We verified using `SnapPy` and `SageMath` (see Appendix) that $V_{B(010101)} = V_{B(101010)}$ (expected, as one is the orientation reversal of the other), and this polynomial is unique among 6-component boot links. Thus, if $B(010101) \sim B(b)$, then $b \in \{010101, 101010\}$.

We must show $B(010101) \not\sim B(101010)$. If they were equivalent, $B(010101)$ would admit an intrinsic symmetry $(1, -1, \ldots, -1, \pi)$, as the isotopy reverses all orientations. But Fact 8.7 states the symmetry group is trivial. Thus, they are not equivalent, so $b = a$.

(2) Since $b = a$, $\mathcal{I}$ is a self-isotopy preserving orientations. Thus $(1, 1, \ldots, 1, \pi)$ is an intrinsic symmetry. By Fact 8.7, $\pi = \iota$. □

We prove the equivalent formulation of Lemma 8.5 (Lemma 8.9), using Observation 8.3.

Lemma 8.9 (([27]) Equivalent to Lemma 8.5)**.** *Let a be an oscillating word of length $n \geqslant 6$. If $B(a) \sim B(b)$ via isotopy $\mathcal{I}$, then,*

(1) the induced permutation is ι; and

(2) $b = a$.

Proof. We use induction on n. Claim 8.8 is the base case $n = 6$. Assume it holds for length $m \geqslant 6$, and consider length $m + 1$.

Let $a = a_1 \cdots a_{m+1}$ be oscillating, $B(a) \sim B(b)$ via $\mathcal{I}$ with permutation π.

Consider the sublinks $B(a)_{1,\ldots,m}$ and $B(a)_{2,\ldots,m+1}$. By Observation 8.3 and the induction hypothesis (Part 1), the permutation induced by $\mathcal{I}$ on the first sublink is ι. This implies $\pi(1) < \cdots < \pi(m)$. Similarly, the permutation induced on the second sublink is ι, implying $\pi(2) < \cdots < \pi(m+1)$. Combining these yields $\pi(1) < \cdots < \pi(m+1)$, so $\pi = \iota$. (1) holds.

Since $\pi = \iota$, $\mathcal{I}$ maps $B(a)_{1,\ldots,m}$ to $B(b)_{1,\ldots,m}$ (†) and $B(a)_{2,\ldots,m+1}$ to $B(b)_{2,\ldots,m+1}$ (‡). By the induction hypothesis (Part 2), (†) implies $b_1 \cdots b_m = a_1 \cdots a_m$, and (‡) implies $b_2 \cdots b_{m+1} = a_2 \cdots a_{m+1}$. Combining these shows $b = a$. (2) holds. □

8.5 Remarks on Unoriented Links

The results in Part III focused on oriented links. We briefly discuss the implications for unoriented links. Let $[\![\mathcal{L}^+(\mathscr{A})]\!]$ be the number of non-equivalent positive *unoriented* links projecting to $\mathscr{A}$.

An oriented link L is *reversible* if it is equivalent to itself with the orientation of all components reversed ($\overline{L}$). If L is not reversible, then L and $\overline{L}$ represent the same unoriented link but are distinct as oriented links.

For the unavoidable arrangements, it can be shown that the proportion of reversible links is asymptotically negligible. This implies that, asymptotically, almost every equivalence class of unoriented links corresponds to two distinct equivalence classes of oriented links (the link and its reverse). Therefore, the number of non-equivalent unoriented links is asymptotically half the number of non-equivalent oriented links.

Theorem 8.10. *([27]) The asymptotic estimates for unoriented links are:*

$$[\![\mathcal{L}^+(\mathscr{R}_n)]\!] = \big(\frac{1}{8} + o(n)\big) \cdot 2^n.$$

$$[\![\mathcal{L}^+(\mathscr{B}_n)]\!] = \big(\frac{1}{2} + o(n)\big) \cdot 2^n.$$

$$[\![\mathcal{L}^+(\mathscr{F}_n)]\!] = \big(\frac{1}{4n} + o(n)\big) \cdot 2^n.$$

Part IV

Conclusions

Chapter 9

Conclusion

In this thesis we explored a complex interface between knot theory and graph theory, specifically investigating how the combinatorial properties of a projection constrain the topological properties of the links it represents. By tackling two distinct but related problems: the characterization of a specific link's projections and the enumeration of links arising from specific projection families we have contributed new tools and results to the theory of link projections.

9.1 Summary of Contributions

9.1.1 Characterization of L6n1

In Part II, we provided a complete characterization of the regular projections of the link $L6n1$. We proved that the necessary condition of being pairwise crossing is also sufficient (Theorem 1.1). This result was achieved through a detailed combinatorial characterization involving reduction operations (shortcutting and simplifying a Θ) and the identification of the two fundamental irreducible projections. This result also enabled the characterization of links related to $L6n1$ under the Taniyama relation.

This result is significant for several reasons. First, it validates the intuition that for any projection, no matter its complexity, the pairwise crossing condition is the *only* obstruction to realization.

Second, the methodology developed here, specifically the rigorous classification of irreducible projections provides a robust framework for attacking similar problems. The proof did not rely on ad-hoc arguments but on a systematic reduction of infinite graphs to a finite set (the two projections P_1 and P_2). This approach allowed us to place $L6n1$ within Taniyama's partial order, identifying its minors and showing that it is majorized by any link with pairwise linked components.

9.1.2 Prolificity of Unavoidable Arrangements

In Part III, we analyzed the prolificity of shadows that are arrangements of pseudocircles, focusing on the three unavoidable families. We established asymptotic estimates for the number of non-equivalent positive oriented links generated by the ring, boot, and flower arrangements (Theorems 1.2, 1.3, and 1.4).

The results revealed significant differences in their prolificity, driven by the underlying symmetries of the arrangements. The boot arrangement is maximally prolific asymptotically, while the ring and flower arrangements generate fewer unique links due to their respective $\mathbb{Z}_2 \times \mathbb{Z}_2$

and dihedral symmetries.

Our main asymptotic results for the number of non-equivalent positive oriented links are:

- **Ring Arrangement:** $\sim \frac{1}{4}2^n$. The four-fold symmetry stems from the ability to rotate the link spatially by 180° around horizontal and vertical axes (corresponding to word reversal and negation).
- **Boot Arrangement:** $\sim 1 \cdot 2^n$. The "boot" structure breaks all spatial symmetries. Consequently, almost every orientation of the pseudocircles yields a topologically distinct positive link.
- **Flower Arrangement:** $\sim \frac{1}{2n}2^n$. The cyclic symmetry of the flower arrangement induces a dihedral action on the binary words, resulting in equivalence classes of size $2n$.

These results provide a quantitative measure of profilicity for these shadows. The fact that the Boot arrangement is asymptotically $4n$ times more prolific than the Flower arrangement (for large n) highlights combinatorial differences of the projections. Furthermore, because these three families are *unavoidable* in large arrangements of pseudocircles, our results essentially shows a rich diversity of links found within any sufficiently large arrangement.

9.2 Future Directions

The results presented in this thesis open several problems for further research.

1. Extending the Characterization to Other Links: The success of the reduction method for $L6n1$ suggests it could be applied to other pairwise linked components. A natural next candidate is the family of Brunnian links, or links with more than three components. Is the condition "every sub-collection of k components must cross" sufficient for realizing specific n-component links? The classification of irreducible projections for 4-component graphs would be significantly more involved, but the logic of reduction operations remains valid.

2. Non-Positive Links in Arrangements: Our asymptotic analysis was restricted to *positive* links. This restriction was crucial because it allowed us to use the strong constraints of positive diagrams. Relaxing this condition to allow arbitrary crossings would likely increase the number of equivalent links. Determining the asymptotic count for general links on $\mathscr{R}_n$ or $\mathscr{F}_n$ remains a challenging open problem.

3. Prolificity of special projections: We characterized the projection of $L6n1$. The inverse problem is also compelling: given a class of projection for example the projection with connectivity k, what is the set of links that can be obtained from these projections.

In conclusion, this thesis demonstrates that the boundary between combinatorics and topology is a fertile ground for discovery. Whether we are reducing a complex projection onto a simpler one or counting the equivalence classes of links that arise from a projection, the interplay of links and their projections continues to yield deep mathematical insights. These results contribute to the broader understanding of how the combinatorial structure of a link projection demarcates the topological properties of the links it can represent.

Appendix

The Jones polynomials for the 16 four-component ring links, the 64 six-component boot links, and the 64 six-component flower links are tabulated in [27] , respectively. These calculations form the necessary foundation for the proofs of Claims 6.7, 8.8, and 7.11.

We computed the Jones polynomials of all these links using `SnapPy` [8] and `SageMath` [34]. Specifically, for every link L, we utilized the PLink editor within `SnapPy` [8] to generate its graphical representation and extract the corresponding Planar Diagram (PD) code. Utilizing this PD representation as input, we then executed computations in `SageMath` [34] to determine the Jones polynomial of L.

List of Figures

Bibliography

[1] The Thistlethwaite Link Table. `http://katlas.org/wiki/The_Thistlethwaite_Link_Table`. Accessed: 2022-08-25.

[2] C. Adams. *The knot book. An elementary introduction to the mathematical theory of knots*. Providence, RI. American Mathematical Society, 2004.

[3] A. Alba, S. Ramírez, and G. Salazar. Regular projections of the link $L6n1$. *J. Knot Theory Ramifications*, 32(1):Paper No. 2350006, 23, 2023.

[4] M. Berglund, J. Cantarella, M. P. Casey, E. Dannenberg, W. George, A. Johnson, A. Kelley, A. LaPointe, M. Mastin, J. Parsley, J. Rooney, and R. Whitaker. Intrinsic symmetry groups of links with 8 and fewer crossings. *Symmetry*, 4(1):143–207, 2012.

[5] J. Cantarella, J. Cornish, M. Mastin, and J. Parsley. The 27 possible intrinsic symmetry groups of two-component links. *Symmetry*, 4(1):129–142, 2012.

[6] J. Cantarella, A. Henrich, E. Magness, O. O'Keefe, K. Perez, E. Rawdon, and B. Zimmer. Knot fertility and lineage. *J. Knot Theory Ramifications*, 26(13):1750093, 20, 2017.

[7] J. Cantarella, A. Henrich, E. Magness, O. O'Keefe, K. Perez, E. Rawdon, and B. Zimmer. Knot fertility and lineage. *J. Knot Theory Ramifications*, 26(13):1750093, 20, 2017.

[8] M. Culler, N. M. Dunfield, M. Goerner, and J. R. Weeks. SnapPy, a computer program for studying the geometry and topology of 3-manifolds. Available at `http://snappy.computop.org` (16/10/2019).

[9] T. Endo, T. Itoh, and K. Taniyama. A graph-theoretic approach to a partial order of knots and links. *Topology Appl.*, 157(6):1002–1010, 2010.

[10] C. Even-Zohar, J. Hass, N. Linial, and T. Nowik. Universal knot diagrams. *J. Knot Theory Ramifications*, 28(7):1950031, 30, 2019.

[11] C. Even-Zohar, J. Hass, N. Linial, and T. Nowik. Universal knot diagrams. *J. Knot Theory Ramifications*, 28(7):1950031, 30, 2019.

[12] S. Felsner and M. Scheucher. Arrangements of pseudocircles: On circularizability. *Discrete Comput. Geom.*, 64(3):776–813, 2020.

[13] R. Hanaki. Regular projections of knotted double-handcuff graphs. *J. Knot Theory Ramifications*, 18(11):1475–1492, 2009.

[14] R. Hanaki. Pseudo diagrams of knots, links and spatial graphs. *Osaka J. Math.*, 47(3):863–883, 2010.

[15] R. Hanaki. Trivializing number of knots. *J. Math. Soc. Japan*, 66(2):435–447, 2014.

[16] R. Hanaki. On scannable properties of the original knot from a knot shadow. *Topology Appl.*, 194:296–305, 2015.

[17] R. Hanaki. On fertility of knot shadows. *J. Knot Theory Ramifications*, 29(11):2050080, 6, 2020.

[18] R. Hanaki and M. Nakamura. A note on closed 3-braid knot shadows. *J. Knot Theory Ramifications*, 32(2):21, 2023. Id/No 2350014.

[19] S. R. Henry and J. R. Weeks. Symmetry groups of hyperbolic knots and links. *Journal of Knot Theory and Its Ramifications*, 01(02):185–201, 1992.

[20] Y. Huh and K. Taniyama. Identifiable projections of spatial graphs. *J. Knot Theory Ramifications*, 13(8):991–998, 2004.

[21] N. Ito and Y. Takimura. $(1,2)$ and weak $(1,3)$ homotopies on knot projections. *J. Knot Theory Ramifications*, 22(14):1350085, 14, 2013.

[22] T. Ito. A note on knot fertility. *Kyushu J. Math.*, 75(2):273–276, 2021.

[23] J. H. Lee and G. T. Jin. Link diagrams realizing prescribed subdiagram partitions. *Kobe J. Math.*, 18(2):199–202, 2001.

[24] C. Livingston. Intrinsic symmetry groups of links. *Algebr. Geom. Topol.*, 23(5):2347–2368, 2023.

[25] C. Medina, J. Ramírez-Alfonsín, and G. Salazar. On the number of unknot diagrams. *SIAM J. Discrete Math.*, 33:306–326, 2019.

[26] C. Medina, J. Ramírez-Alfonsín, and G. Salazar. The unavoidable arrangements of pseudocircles. *Proc. Amer. Math. Soc.*, 147(7):3165–3175, 2019.

[27] C. Medina, S. Ramírez, J. L. Ramírez-Alfonsín, and G. Salazar. Positive links with arrangements of pseudocircles as shadows. *Topology and its Applications*, 354:108999, 2024.

[28] C. Medina and G. Salazar. The knots that lie above all shadows. *Topology Appl.*, 268:106922, 13, 2019.

[29] C. Medina and G. Salazar. When can a link be obtained from another using crossing exchanges and smoothings? *Topology Appl.*, 260:13–22, 2019.

[30] J. H. Przytycki and K. Taniyama. Almost positive links have negative signature. *J. Knot Theory Ramifications*, 19(2):187–289, 2010.

[31] Y. Takimura. Regular projections of the knot 6_2. *J. Knot Theory Ramifications*, 27(14):1850081, 31, 2018.

[32] K. Taniyama. A partial order of knots. *Tokyo J. Math.*, 12(1):205–229, 1989.

[33] K. Taniyama. A partial order of links. *Tokyo J. Math.*, 12(2):475–484, 1989.

[34] The Sage Developers. *SageMath, the Sage Mathematics Software System (Version 10.0)*, 2023. `https://www.sagemath.org`.

[35] W. C. Whitten, Jr. Symmetries of links. *Trans. Amer. Math. Soc.*, 135:213–222, 1969.